Eur. Phys. J. C 21, 319–338 (2001)
Digital Object Identifier (DOI) 10.1007/s100520100744

THE EUROPEAN PHYSICAL JOURNAL C

Heavy-light current correlators at order α_s^2 in QCD and HQET

K.G. Chetyrkin[1,2,*], M. Steinhauser[3]

[1] Fakultät für Physik, Universität Freiburg, 79104 Freiburg, Germany
[2] Institut für Theoretische Teilchenphysik, Universität Karlsruhe, 76128 Karlsruhe, Germany
[3] II. Institut für Theoretische Physik, Universität Hamburg, 22761 Hamburg, Germany

Received: 19 June 2001 /
Published online: 10 August 2001 –

Abstract. The non-diagonal correlators of vector and scalar currents are considered at three-loop order in QCD. The full mass dependence is computed in the case where one of the quarks is massless and the other one carries mass M. We exploit the decoupling relations between the full theory and the heavy quark effective theory (HQET) in order to obtain the logarithmic parts of the leading threshold terms. With the help of conformal mapping and Padé approximation numerical estimates for the non-logarithmic terms are extracted which in turn lead to a prediction of the correlator in HQET at order α_s^2. As applications of the vector and scalar correlator we consider the single-top-quark production via the process $q\bar{q} \to t\bar{b}$ and the decay rate of a charged Higgs boson into hadrons, respectively. In both cases the computed NLO corrections are shown to be numerically much less important than the leading ones. On the contrary, the NLO order QCD corrections to the HQET sum rule for the leptonic decay rate of a heavy-light meson proves to be comparable to the leading one.

1 Introduction

In QCD the correlator of two currents is very often a central object from which important physical consequences can be deduced. In particular, in case the coupling of the currents is diagonal physical observables like e^+e^- annihilation into hadrons and the decay of the Z boson are obtained from the vector and axial-vector current correlators. Furthermore, total decay rates of CP even or CP odd Higgs bosons can be obtained by considering the scalar and pseudo-scalar current densities, respectively. For these cases the results are available up to order α_s^2 taking into account the full quark mass dependence both for the non-singlet [1] and singlet [2] correlators.

In this work we want to extend the techniques developed in [1,2] to the situation where the coupling of the external currents to quarks is non-diagonal. In particular we compute the three-loop correlators of currents which couple to two different quark flavors. To be precise we want to consider the case where one of the quarks is massless and the other carries mass M. In this limit the vector (scalar) and axial-vector (pseudo-scalar) correlators coincide. A short account of our results has been presented in [3]. In this paper the details of the calculation are given and explicit expressions for intermediate results are provided which might be useful for other applications.

The main aim of this work is to obtain results which are valid for arbitray values of the quark mass, M, respectively the ratio q^2/M^2 where q is the external momentum of the correlator. Very often the knowledge of the full mass dependence is not necessary. E.g., in high energy experiments where the center-of-mass energy, $s^{1/2}$, is much larger than the mass of the quarks, the latter can often be neglected or an expansion in $M/s^{1/2}$ is sufficient to describe the data. However, there are situations where the full dependence on M and $s^{1/2}$ is required. One can, e.g., think on the high precision which meanwhile has been reached at LEP (CERN), SLC (SLAC) or TEVATRON (Fermilab) or on situations where the center-of-mass energy is of the same order of magnitude as the quark masses. In particular for threshold phenomena the masses are important and the full dependence is desirable.

Concerning the physical applications of the non-diagonal vector and axial-vector correlators we have in mind properties connected to the W boson. With the results of this paper at hand a certain (gauge invariant) class of corrections to the Drell–Yan process becomes available. In particular we have in mind the production of a quark pair through the decay of a virtual W boson generated in $p\bar{p}$ collisions. The absorptive part of the considered correlator is directly related to the decay width of the (highly virtual) W bosons into quark pairs and gluons. Of particular interest in this connection is the single-top-quark production via the process $q\bar{q} \to t\bar{b}$. The imaginary part of the transversal W boson polarization function constitutes a gauge invariant and finite contribution of $\mathcal{O}(\alpha_s^2)$.

* *Permanent address:* Institute for Nuclear Research, Russian Academy of Sciences, 60th October Anniversary Prospect 7a, Moscow 117312, Russia

As an application of the scalar and pseudo-scalar current correlator we want to mention the decay of a charged Higgs boson which occurs in extensions of the standard model (SM). The corrections provided in this paper describe the total decay rate into a massive and a massless quark.

Another important application of the non-diagonal vector and scalar current correlator is connected to the corresponding meson decay constant. Within HQET it is related to the imaginary part of the effective current correlator, i.e. the spectral density, evaluated near threshold. As the current in the effective theory does not depend on the γ-matrix structure it can be derived both from the vector and the scalar correlator of the full theory which are evaluated in this work. The corresponding analysis at order α_s has been performed in [4,5] with the conclusion that the determination of the B meson decay constant suffers from large perturbative corrections. We show in this paper that the corrections of order α_s^2 are also sizeable.

This paper is organized as follows. In Sect. 2 we provide useful definitions and describe the method we use for the computation. The connection between the effective and full theory is established in Sect. 3. In Sect. 4 we present explicit results for the moments of the vector and scalar current correlator and discuss the results for the corresponding spectral densities in the full theory. Afterwards, in Sect. 5, the procedure is discussed which allows for the extraction of threshold information from our results. This can be translated to the effective theory which provides a result for the spectral density in the effective theory up to order α_s^2. Finally, in Sect. 6, we discuss some physical applications and present our conclusions. The appendix contains the analytical results of the low- and high-energy moments for the vector and scalar correlator.

2 Conformal mapping and Padé approximation

In this section we want to describe the method we use for the computation of the current correlators in full QCD. Let us start with some definitions.

In the vector case the polarization function is defined through

$$(-q^2 g_{\mu\nu} + q_\mu q_\nu)\Pi^v(q^2) + q_\mu q_\nu \Pi_L^v(q^2) = \mathrm{i}\int \mathrm{d}x \mathrm{e}^{\mathrm{i}qx}\langle 0|T j_\mu^v(x) j_\nu^{v\dagger}(0)|0\rangle, \tag{1}$$

with $j_\mu^v = \bar{\psi}_1\gamma_\mu\psi_2$. Only the transversal part $\Pi^v(q^2)$ will be considered in the following. The definition of the scalar polarization function reads

$$q^2\Pi^s(q^2) = \mathrm{i}\int \mathrm{d}x \mathrm{e}^{\mathrm{i}qx}\langle 0|T j^s(x) j^{s\dagger}(0)|0\rangle, \tag{2}$$

with $j^s = (m(\mu)/M)\bar{\psi}_1\psi_2$ where $m(\mu)$ is the $\overline{\mathrm{MS}}$ and M the on-shell mass of ψ_2. ψ_1 we consider to be massless. Thus we will identify ψ_1 with q, the massless quark, and ψ_2 with Q which is supposed to be a heavy quark of mass M. This will become relevant later on when we consider the effective theory. Throughout this paper we consider anticommuting γ_5 which is justified as for $\psi_1 \neq \psi_2$ only non-singlet diagrams contribute. As a consequence the axial-vector (pseudo-scalar) correlator coincides with the vector (scalar) one.

It is convenient to introduce the dimensionless variable

$$z = \frac{q^2}{M^2}, \tag{3}$$

where M refers to the pole mass. For the overall normalization of $\Pi^\delta(q^2)$ ($\delta = v, s$) we adopt the QED-like conditions $\Pi^\delta(0) = 0$.

The physical observables $R(s)$ are related to $\Pi(q^2)$ through

$$R^v(s) = 12\pi\mathrm{Im}[\Pi^v(q^2 = s + \mathrm{i}\epsilon)], \tag{4}$$

$$R^s(s) = 8\pi\mathrm{Im}[\Pi^s(q^2 = s + \mathrm{i}\epsilon)], \tag{5}$$

where the use of the variables

$$x = \frac{M}{\sqrt{s}}, \quad v = \frac{1-x^2}{1+x^2}, \tag{6}$$

turns out to be useful to describe the high energy and threshold region, respectively.

The expansion of Π^δ in terms of α_s reads ($\delta = v, s$)

$$\Pi^\delta = \Pi^{(0),\delta} + \frac{\alpha_s^{(n_f)}(\mu)}{\pi} C_F \Pi^{(1),\delta} + \left(\frac{\alpha_s^{(n_f)}(\mu)}{\pi}\right)^2 \Pi^{(2),\delta} + \mathcal{O}(\alpha_s^3). \tag{7}$$

It is convenient to further decompose the three-loop term according to the color structure

$$\Pi^{(2),\delta} = C_F^2\Pi_{FF}^{(2),\delta} + C_A C_F \Pi_{FA}^{(2),\delta} + C_F T n_l \Pi_L^{(2),\delta} + C_F T \Pi_{FH}^{(2),\delta}, \tag{8}$$

where analogous formulae hold for $R(s)$ and also for the corresponding quantities in the effective theory which we will define below. $C_F = (N_c^2 - 1)/(2N_c)$ and $C_A = N_c$ are the eigenvalues of the quadratic Casimir operator of the fundamental and adjoint representation, respectively, and $T = 1/2$ is the index of the fundamental representation. In (8) $\Pi_{FF}^{(2),\delta}$ corresponds to the abelian part already present in QED whereas $\Pi_{FA}^{(2),\delta}$ represents the non-abelian structure. The remaining two structures correspond to the fermionic contributions where n_l counts the number of massless quarks and $n_f = n_l + 1$ is the total number of active quark flavors.

For later convenience we want to list the exact expressions for the Born results and the corrections of order α_s [6–10]. In the vector case we have

$$R^{(0),v}(s) = \frac{N_c}{2}(1-x^2)^2(2+x^2),$$

$$R^{(1),v}(s) = \frac{3N_c}{4}\left\{1 - \frac{5x^2}{2} + \frac{2x^4}{3} + \frac{5x^6}{6} + \frac{1}{3}x^2\right.$$

$$\times(-5-4x^2+5x^4)\ln(x^2)-\frac{1}{3}(1-x^2)^2$$
$$\times(4+5x^2)\ln(1-x^2)-\frac{2}{3}(1-x^2)^2(2+x^2)$$
$$\times\left[-\ln\left(\frac{x^2}{1-x^2}\right)\ln(1-x^2)\right.$$
$$\left.+\ 2\mathrm{Li}_2\left(-\frac{x^2}{1-x^2}\right)\right]\Bigg\}. \qquad (9)$$

Correspondingly, the scalar current correlators read

$$R^{(0),s}(s)=N_c(1-x^2)^2,$$
$$R^{(1),s}(s)=-\frac{N_c}{2}(1-x^2)\Bigg\{-(3-7x^2+2x^4)\ln(x^2)$$
$$+(1-x^2)\left[-\frac{9}{2}+(5-2x^2)\ln(1-x^2)\right]$$
$$+2(1-x^2)\left[-\ln\left(\frac{x^2}{1-x^2}\right)\ln(1-x^2)\right.$$
$$\left.+\ 2\mathrm{Li}_2\left(-\frac{x^2}{1-x^2}\right)\right]\Bigg\}. \qquad (10)$$

A complete analytical computation of $\Pi^\delta(q^2)$ at three-loop order or its imaginary part is currently not feasible. The method we use for the computation of the diagrams has successfully been applied to several physical quantities (see, e.g., [11,1,2,12]). It allows for the computation of a semi-numerical approximation for $\Pi(q^2)$. The aim is the reconstruction of the function $\Pi(q^2)$ from the knowledge of some moments for $z\to 0$ and $z\to-\infty$ and additional partial information about the behavior of $R(s)$ for $s\to M^2$. For convenience we briefly summarize the different steps which have to be performed for the individual pieces of (7) and (8). In the following we generically write $\Pi(q^2)$.
(1) Compute as many moments as possible for small and large z. In our case the expansion for $z\to 0$ reduces to a simple Taylor series of the Feynman diagrams in the external momentum. For $z\to-\infty$, however, the rules of asymptotic expansion [13] have to be applied. Thus in this limit besides the power corrections there are logarithmic terms in z.
(2) The information known about the imaginary part $R(s)$ for $s\to M^2$ has to be transformed to a function $\Pi^{\rm thr}(q^2)$. Afterwards $\Pi^{\rm thr}(q^2)$ has to be expanded in the limits $z\to 0$ and $z\to-\infty$ and the moments have to be subtracted from the ones of $\Pi(q^2)$. It is important to construct $\Pi^{\rm thr}(q^2)$ in such a way that its expansion for $z\to 0$ is analytical. In this way the information about the logarithmic part of $\Pi^{\rm thr}(q^2)$ can be incorporated.
(3) Construct a function $\Pi^{\log}(q^2)$ in such a way that the combination

$$\tilde\Pi(q^2)\equiv\Pi(q^2)-\Pi^{\rm thr}(q^2)-\Pi^{\log}(q^2) \qquad (11)$$

is polynomial in z and $1/z$, i.e. in the small and high energy region. Furthermore no logarithmic singularities may be introduced at threshold.
(4) Perform a conformal mapping. The change of variables [14]

$$z=\frac{4\omega}{(1+\omega)^2}, \qquad (12)$$

maps the z plane into the interior of the unit circle of the w plane. Thereby the cut $[1,\infty)$ is mapped to the perimeter.
(5) Define [2]

$$P_n(\omega)=\frac{(4\omega)^{n-1}}{(1+\omega)^{2n}} \qquad (13)$$
$$\times\left(\tilde\Pi(q^2)-\sum_{j=0}^{n-1}\frac{1}{j!}\left(\frac{\mathrm{d}^j}{\mathrm{d}(1/z)^j}\tilde\Pi(q^2)\Big|_{z=-\infty}\right)\frac{(1+\omega)^{2j}}{(4\omega)^j}\right),$$

where for $\tilde\Pi(q^2)$ the terms up to order $1/z^n$ must be known. The available information transforms into $P_n(-1)$ and $P_n^{(k)}(0),(k=0,1,\ldots,n+n_0-1)$, where n_0 is the number of moments for $z\to 0$.
(6) In the last step a Padé approximation is performed for the function $P_n(\omega)$. This means that $P_n(\omega)$ is represented through a function

$$[i/j](\omega)=\frac{a_0+a_1\omega+\cdots+a_i\omega^i}{1+b_1\omega+\cdots+b_j\omega^j}, \qquad (14)$$

where the number of coefficients on the r.h.s. depend on the amount of information available for $P_n(\omega)$.

Once an approximation for $P(\omega)$ is known the above steps have to be inverted in order to obtain the function $\Pi(q^2)$.

Due to the structure of (14) some Padé approximants develop poles inside the unit circle ($|\omega|\le 1$). In general we will discard such results in the following. In some cases, however, the pole coincides with a zero of the numerator up to several digits accuracy. These Padé approximations will be taken into account in constructing our results. To be precise: in addition to the Padé results without any poles inside the unit circle, we will use the ones where the poles are accompanied by zeros within a circle of radius 0.01, and the distance between the pole and the physically relevant point $q^2/M^2=1$ is larger than 0.1.

3 Current correlator in the effective theory

The computation of the current correlators is performed in the full theory. In this section the connection to the correlator in the HQET is described. This connection is exploited to obtain the leading logarithmic terms of $R^v(s)$ and $R^s(s)$ at threshold.

In the effective theory we denote the $\overline{\rm MS}$ renormalized current which couples to a massive and a massless quark by

$$\tilde j_\Gamma=\bar q\Gamma\tilde Q, \qquad (15)$$

with $\Gamma\in\{1,\gamma^\mu,\mathrm{i}\gamma_5,\gamma^\mu\gamma_5\}$. The light quark flavor q is identical in the full and the effective theory which is not

true for the heavy one as indicated by the tilde. In the effective theory $\tilde{Q}$ is considered as a static quark which fulfills the relation

$$\tilde{Q} = \gamma_0 \tilde{Q}. \tag{16}$$

Due to this condition the set of γ matrices can be divided into two groups: one which commutes ($\{\mathrm{i}\gamma_5, \gamma_j\}, j = 1,2,3$) and one which anti-commutes ($\{1, \gamma_j\gamma_5\}$) with γ_0.

Let us next consider the corresponding correlators which are defined in analogy to (1) and (2)

$$\tilde{\Pi}_{\Gamma_1,\Gamma_2}(q_0) = \mathrm{i}\int \mathrm{d}x \mathrm{e}^{\mathrm{i}qx} \langle 0|T\tilde{j}_{\Gamma_1}(x)\tilde{j}^\dagger_{\Gamma_2}(0)|0\rangle. \tag{17}$$

They only depend on the zeroth component q_0 as due to the Feynman rules of HQET in coordinate space one has $\langle 0|T\tilde{j}_\Gamma(x)\tilde{j}^\dagger_\Gamma(0)|0\rangle \sim \delta(\vec{x})$. Furthermore, in our case where only one of the quarks is massive, one can write all correlators in terms of $\tilde{\Pi}(q_0) \equiv \tilde{\Pi}_{1,1}(q_0)$. It is possible to show that the following equations hold[1]

$$\begin{aligned}
\tilde{\Pi}_{\mathrm{i}\gamma_5,\mathrm{i}\gamma_5}(q_0) &= \tilde{\Pi}(q_0),\\
\tilde{\Pi}_{\gamma_i,\gamma_j}(q_0) &= \delta_{ij}\tilde{\Pi}(q_0),\\
\tilde{\Pi}_{\gamma_i\gamma_5,\gamma_j\gamma_5}(q_0) &= \delta_{ij}\tilde{\Pi}(q_0).
\end{aligned} \tag{18}$$

Thus in HQET there is only one independent correlator, $\tilde{\Pi}(q_0)$, which will be considered in the following. The corresponding current will be denoted by $\tilde{j}$.

The relation between $\tilde{j}$ and j^δ ($\delta = v, s$) has been computed in [15] up to order α_s^2. For $\mu = M$ it can be written in the form

$$j^\delta = C_\delta(M)\tilde{j}, \tag{19}$$

where the decoupling constants $C_\delta(M)$ are given by

$$\begin{aligned}
C_v(M) = 1 &- C_F\frac{\alpha_s^{(n_f)}(M)}{\pi} + \left(\frac{\alpha_s^{(n_f)}(M)}{\pi}\right)^2 \\
&\times\left[C_F^2\left(\frac{1453}{768} - \frac{173}{48}\zeta_2 + \frac{7}{2}\zeta_2\ln 2 - \frac{11}{8}\zeta_3\right)\right.\\
&+C_FC_A\left(-\frac{6821}{2304} + \frac{21}{16}\zeta_2 - \frac{7}{4}\zeta_2\ln 2 + \frac{9}{16}\zeta_3\right)\\
&\left.+C_FTn_l\left(\frac{445}{576} + \frac{1}{4}\zeta_2\right) + C_FT\left(\frac{709}{576} - \frac{5}{6}\zeta_2\right)\right],
\end{aligned} \tag{20}$$

$$\begin{aligned}
C_s(M) = 1 &+ \frac{C_F}{2}\frac{\alpha_s^{(n_f)}(M)}{\pi} + \left(\frac{\alpha_s^{(n_f)}(M)}{\pi}\right)^2 \\
&\times\left[C_F^2\left(\frac{369}{256} + \frac{15}{16}\zeta_2 - \frac{3}{2}\zeta_2\ln 2 - \frac{1}{8}\zeta_3\right)\right.\\
&+C_FC_A\left(\frac{1351}{768} - \frac{3}{16}\zeta_2 + \frac{3}{4}\zeta_2\ln 2 - \frac{1}{16}\zeta_3\right)\\
&\left.+C_FTn_l\left(-\frac{95}{192} - \frac{1}{4}\zeta_2\right) + C_FT\left(\frac{169}{192} - \frac{1}{2}\zeta_2\right)\right],
\end{aligned} \tag{21}$$

[1] This is true only if no power suppressed non-perturbative corrections are taken into account, what is implicitly understood throughout the present paper

with $\zeta_2 = \pi^2/6$ and $\zeta_3 \approx 1.202057$. The superscript attached to α_s defines the number of active flavors. $\tilde{j}$ is still defined with n_f active flavors. The transition to a theory with only n_l active flavors is achieved through

$$\tilde{j} = \tilde{C}(M)\tilde{j}', \tag{22}$$

with [16]

$$\tilde{C}(M) = 1 + \frac{89}{576}C_FT\left(\frac{\alpha_s^{(n_l)}(M)}{\pi}\right)^2, \tag{23}$$

where again $\mu = M$ has been adopted. In analogy to (17) and (18) one can define polarization functions also in the primed theory. Again there is only one which is independent. It will be denoted by $\tilde{\Pi}'(q_0)$ which only depends on the massless quark flavors. Thus besides the renormalization scale μ there is only one more dimensionful quantity which in the framework of HQET is usually chosen to be $\omega = s^{1/2} - M$. As a consequence the renormalization group equation for $\tilde{j}'$ takes the simple form

$$\mu^2\frac{\mathrm{d}}{\mathrm{d}\mu^2}\tilde{j}' = \tilde{\gamma}'\tilde{j}', \tag{24}$$

with [17]

$$\begin{aligned}
\tilde{\gamma}' = C_F\frac{3}{8}\frac{\alpha_s^{(n_l)}}{\pi} + \left(\frac{\alpha_s^{(n_l)}}{\pi}\right)^2 &\left[-C_F^2\left(\frac{5}{64} - \frac{1}{2}\zeta_2\right)\right.\\
&\left.- C_AC_F\left(-\frac{49}{192} + \frac{1}{8}\zeta_2\right) - C_FTn_l\frac{5}{48}\right] + \mathcal{O}(\alpha_s^3).
\end{aligned} \tag{25}$$

Note that the primed quantities only depend on $\alpha_s^{(n_l)}$. This allows for a simple reconstruction of the logarithms $\ln(\mu^2/\omega^2)$ at $\mathcal{O}(\alpha_s^2)$ of $\tilde{R}'$ defined through

$$\tilde{R}'(\omega) = 2\pi\mathrm{Im}[\tilde{\Pi}'(q_0)]|_{q^2=s+\mathrm{i}\epsilon,\omega=\sqrt{s}-M}. \tag{26}$$

Once they are at hand (20), (21) and (23) can be used to predict the logarithms of R^v and R^s at threshold via the relations

$$\begin{aligned}
R^v(s) &= 6[C_v(M)\tilde{C}(M)]^2\frac{v^2}{\omega^2}\tilde{R}' + \mathcal{O}(v^3),\\
R^s(s) &= 4\left[\frac{m(M)}{M}C_s(M)\tilde{C}(M)\right]^2\frac{v^2}{\omega^2}\tilde{R}' + \mathcal{O}(v^3),
\end{aligned} \tag{27}$$

where it is understood that ω is expressed in terms of v via the relation

$$1 - \frac{\omega}{M} = \sqrt{\frac{1-v}{1+v}}, \tag{28}$$

an expansion for $v \to 0$ is performed and only the leading term is kept.

At this point we want to mention that the developed formalism – in particular the decoupling relations (19) and (23) – only applies to the imaginary part. For the polarization function one would have to take into account additional contributions.

The procedure described above determines the logarithmic parts of the leading threshold term. They are incorporated into the Padé procedure as described in Sect. 2 (cf. point (2)). Note, that the non-logarithmic part for R^δ are not fixed via this procedure. In Sect. 5 we will extract numerical approximations from our Padé results.

At the end of this section we want to list the available information for $\tilde{R}'(\omega)$. Using (24) and (25) and the $\mathcal{O}(\alpha_s)$ result for $\tilde{R}'$ [4,5] one obtains

$$\begin{aligned}
&\tilde{R}'(\omega) \qquad (29)\\
&= N_c\omega^2\left\{1+\frac{\alpha_s^{(n_l)}(\mu)}{\pi}C_F\right.\\
&\times\left(\frac{17}{4}-\frac{3}{2}\ln 2+2\zeta_2+\frac{3}{4}L_\omega\right)+\left(\frac{\alpha_s^{(n_l)}(\mu)}{\pi}\right)^2\\
&\times\left[C_F^2\left(\tilde{c}_{FF}+\left(\frac{97}{32}-\frac{9}{8}\ln 2+\frac{5}{2}\zeta_2\right)L_\omega+\frac{9}{32}L_\omega^2\right)\right.\\
&+C_AC_F\left(\tilde{c}_{FA}+\left(\frac{141}{32}-\frac{11}{8}\ln 2+\frac{19}{12}\zeta_2\right)L_\omega+\frac{11}{32}L_\omega^2\right)\\
&\left.\left.+C_FTn_l\left(\tilde{c}_{FL}+\left(-\frac{13}{8}+\frac{1}{2}\ln 2-\frac{2}{3}\zeta_2\right)L_\omega-\frac{1}{8}L_\omega^2\right)\right]\right\},
\end{aligned}$$

with $L_\omega=\ln(\mu^2/\omega^2)$. The coefficients $\tilde{c}_{FF}$, $\tilde{c}_{FA}$ and $\tilde{c}_{FL}$ are not known. In Sect. 5 we will provide numerical approximations.

With the help of (27) one obtains the leading terms of R^v and R^s for $v\to 0$. Separated according to the color factors they read ($\mu=M$)

$$\begin{aligned}
&R^{v,\mathrm{thr}}\\
&= N_cv^2\left\{6+\frac{\alpha_s^{(n_f)}(M)}{\pi}C_F\right.\\
&\times\left(\frac{27}{2}+12\zeta_2-9\ln 2-9\ln v\right)+\left(\frac{\alpha_s^{(n_f)}(M)}{\pi}\right)^2\\
&\times\left[C_F^2\left(c_{FF}^v+\left(-\frac{147}{8}-30\zeta_2+\frac{27}{2}\ln 2\right)\ln v+\frac{27}{4}\ln^2 v\right)\right.\\
&+C_AC_F\left(c_{FA}^v+\left(-\frac{423}{8}-19\zeta_2+\frac{33}{2}\ln 2\right)\ln v\right.\\
&\left.+\frac{33}{4}\ln^2 v\right)\\
&+C_FTn_l\left(c_{FL}^v+\left(\frac{39}{2}+8\zeta_2-6\ln 2\right)\ln v-3\ln^2 v\right)\\
&\left.\left.+C_FT\left(\frac{133}{8}-10\zeta_2\right)\right]\right\}, \qquad (30)\\
&R^{s,\mathrm{thr}}\\
&= N_cv^2\left\{4+\frac{\alpha_s^{(n_f)}(M)}{\pi}C_F(13+8\zeta_2-6\ln 2-6\ln v)\right.\\
&+\left(\frac{\alpha_s^{(n_f)}(M)}{\pi}\right)^2\\
&\times\left[C_F^2\left(c_{FF}^s+\left(-\frac{73}{4}-20\zeta_2+9\ln 2\right)\ln v+\frac{9}{2}\ln^2 v\right)\right.\\
&+C_AC_F\left(c_{FA}^s+\left(-\frac{141}{4}-\frac{38}{3}\zeta_2+11\ln 2\right)\ln v\right.\\
&\left.+\frac{11}{2}\ln^2 v\right)\\
&+C_FTn_l\left(c_{FL}^s+\left(13+\frac{16}{3}\zeta_2-4\ln 2\right)\ln v-2\ln^2 v\right)\\
&\left.\left.+C_FT\left(\frac{727}{36}-12\zeta_2\right)\right]\right\}, \qquad (31)
\end{aligned}$$

with $\zeta_2=\pi^2/6$. The smooth behavior proportional to v^2 is a consequence from the fact that $\tilde{R}'$ is, for dimensional reasons, proportional to ω^2. This is in contrast to the diagonal correlators where at order α_s^2 even $1/v$ singularities appear [1]. Note that in (30) and (31) the terms proportional to the color factor C_FT are completely fixed. For later use it is convenient to display explicitly the relations between $\tilde{c}$ and c^δ:

$$\begin{aligned}
c_{FF}^v &= 6\tilde{c}_{FF}-\frac{1427}{64}+18\ln 2-\frac{269}{4}\zeta_2+42\zeta_2\ln 2\\
&\quad -\frac{33}{2}\zeta_3\approx -92.3884+6\tilde{c}_{FF},\\
c_{FA}^v &= 6\tilde{c}_{FA}-\frac{6821}{192}+\frac{63}{4}\zeta_2-21\zeta_2\ln 2+\frac{27}{4}\zeta_3\\
&\approx -25.4483+6\tilde{c}_{FA},\\
c_{FL}^v &= 6\tilde{c}_{FL}+\frac{445}{48}+3\zeta_2\approx +14.2056+6\tilde{c}_{FL}, \qquad (32)\\
c_{FF}^s &= 4\tilde{c}_{FF}-\frac{257}{32}+6\ln 2-\frac{31}{2}\zeta_2+12\zeta_2\ln 2-7\zeta_3\\
&\approx -24.1011+4\tilde{c}_{FF},\\
c_{FA}^s &= 4\tilde{c}_{FA}-\frac{871}{96}+\frac{5}{2}\zeta_2-6\zeta_2\ln 2+\frac{5}{2}\zeta_3\\
&\approx -8.79653+4\tilde{c}_{FA},\\
c_{FL}^s &= 4\tilde{c}_{FL}+\frac{47}{24}+2\zeta_2\approx 5.2482+4\tilde{c}_{FL}. \qquad (33)
\end{aligned}$$

4 Spectral function in full QCD

In this section we discuss the computation of the polarization function in full QCD. Explicit results are given for the imaginary parts which constitute physical quantities. In a first step the input quantities needed for the Padé procedure are provided.

In Fig. 1 typical diagrams are pictured. Altogether roughly 30 contributions have to be considered at three-loop order. Although their number is relatively small we used GEFICOM [18] for the automatic computation. GEFICOM uses QGRAF [19] for the generation of the diagrams. In case an asymptotic expansion has to be applied LMP [20] or EXP [21] are used for the generation of the sub-diagrams. The occurring vacuum diagrams are passed to MATAD [22] and the massless propagator-type diagrams are evaluated to MINCER [23]. More details on the automatic computation of Feynman diagrams can be found in [24].

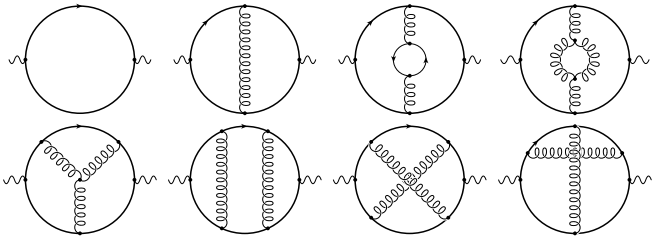

Fig. 1. Sample diagrams contributing to the current correlator of (1) and (2). The straight and loopy lines represent quarks and gluons, respectively. One of the quarks connected to the external current carries mass M whereas the other one is massless

At three-loop order terms up to order z^6 (z^7) could be evaluated for the vector (scalar) correlator in the limit $z \to 0$. For convenience we list below the analytical results for the one- and two-loop correlator up to order z^7 and present the results for the $\Pi^{(2),\delta}$ in the appendix. The analytical results can also be found under the URL http://www-ttp.physik.uni-karlsruhe.de/Progdata/ttp01/ttp01-14. In the low-energy limit we obtain at order α_s^0 and α_s^1

$$\begin{aligned}
\Pi^{(0),v} &= \frac{3}{16\pi^2}\left[+\frac{1}{2}z+\frac{2}{15}z^2+\frac{1}{18}z^3+\frac{1}{35}z^4\right.\\
&\quad\left.+\frac{1}{60}z^5+\frac{2}{189}z^6+\frac{1}{140}z^7\right]+\ldots,\\
\Pi^{(1),v} &= \frac{3}{16\pi^2}\left[+\left(\frac{1}{2}\zeta_2+\frac{25}{48}\right)z+\left(\frac{2}{15}\zeta_2+\frac{5}{18}\right)z^2\right.\\
&\quad+\left(\frac{1}{18}\zeta_2+\frac{503}{3240}\right)z^3+\left(\frac{1}{35}\zeta_2+\frac{1199}{12600}\right)z^4\\
&\quad+\left(\frac{1}{60}\zeta_2+\frac{37883}{604800}\right)z^5+\left(\frac{2}{189}\zeta_2+\frac{23029}{529200}\right)z^6\\
&\quad\left.+\left(\frac{1}{140}\zeta_2+\frac{222433}{7056000}\right)z^7\right]+\ldots, \qquad (34)\\
\Pi^{(0),s} &= \frac{3}{16\pi^2}\left[+\frac{2}{3}z+\frac{1}{6}z^2+\frac{1}{15}z^3+\frac{1}{30}z^4\right.\\
&\quad\left.+\frac{2}{105}z^5+\frac{1}{84}z^6+\frac{1}{126}z^7\right]+\ldots,\\
\Pi^{(1),s} &= \frac{3}{16\pi^2}\left[+\left(\frac{2}{3}\zeta_2+\frac{1}{12}\right)z+\left(\frac{1}{6}\zeta_2+\frac{19}{48}\right)z^2\right.\\
&\quad+\left(\frac{1}{15}\zeta_2+\frac{17}{72}\right)z^3+\left(\frac{1}{30}\zeta_2+\frac{31}{216}\right)z^4\\
&\quad+\left(\frac{2}{105}\zeta_2+\frac{7001}{75600}\right)z^5+\left(\frac{1}{84}\zeta_2+\frac{38113}{604800}\right)z^6\\
&\quad\left.+\left(\frac{1}{126}\zeta_2+\frac{18961}{423360}\right)z^7\right]+\ldots, \qquad (35)
\end{aligned}$$

where the on-shell quark mass M has been used as a parameter.

In the high energy region eight expansion terms could be obtained both in the vector and scalar case. Again we provide in the main text the one- and two-loop results in analytic form and refer for the analytic three-loop terms to the Appendix and to the URL http://www-ttp.physik.uni-karlsruhe.de/Progdata/ttp01/ttp01-14. Using again the on-shell mass the one-and two-loop results read

$$\begin{aligned}
\Pi^{(0),v} &= \frac{3}{16\pi^2}\left[\frac{16}{9}+\frac{8}{3}L_z+(1-4L_z)\frac{1}{z}-2\frac{1}{z^2}\right.\\
&\quad+\left(\frac{4}{3}L_z-\frac{5}{9}\right)\frac{1}{z^3}+\frac{1}{3}\frac{1}{z^4}\\
&\quad\left.+\frac{1}{10}\frac{1}{z^5}+\frac{2}{45}\frac{1}{z^6}+\frac{1}{42}\frac{1}{z^7}\right]+\ldots,\\
\Pi^{(1),v} &= \frac{3}{16\pi^2}\left[\frac{25}{18}+2L_z-4\zeta_3+\frac{4}{9}\zeta_2\right.\\
&\quad+\left(3L_z-6L_z^2-\zeta_2+6\zeta_3-\frac{23}{4}\right)\frac{1}{z}\\
&\quad+(2-6L_z)\frac{1}{z^2}\\
&\quad+\left(-\left(\frac{104}{27}L_z\right)+\frac{40}{9}L_z^2-2\zeta_3+\frac{28}{27}\right)\frac{1}{z^3}\\
&\quad+\left(\frac{31}{9}L_z-\frac{2}{3}L_z^2-\frac{31}{16}\right)\frac{1}{z^4}\\
&\quad+\left(\frac{56}{75}L_z-\frac{1}{5}L_z^2-\frac{1747}{36000}\right)\frac{1}{z^5}\\
&\quad+\left(\frac{7}{25}L_z-\frac{4}{45}L_z^2+\frac{3833}{81000}\right)\frac{1}{z^6}\\
&\quad\left.+\left(\frac{296}{2205}L_z-\frac{1}{21}L_z^2+\frac{322099}{7408800}\right)\frac{1}{z^7}\right]+\ldots, \qquad (36)\\
\Pi^{(0),s} &= \frac{3}{16\pi^2}\left[3+4L_z-8L_z\frac{1}{z}+(-3+4L_z)\frac{1}{z^2}\right.\\
&\quad\left.+\frac{2}{3}\frac{1}{z^3}+\frac{1}{6}\frac{1}{z^4}+\frac{1}{15}\frac{1}{z^5}+\frac{1}{30}\frac{1}{z^6}+\frac{2}{105}\frac{1}{z^7}\right]+\ldots,\\
\Pi^{(1),s} &= \frac{3}{16\pi^2}\left[\frac{19}{4}+6L_z^2+9L_z-6\zeta_3+\zeta_2\right.\\
&\quad+(-7-24L_z^2+12\zeta_3)\frac{1}{z}\\
&\quad+(8-24L_z+24L_z^2-6\zeta_3)\frac{1}{z^2}\\
&\quad+\left(\frac{128}{9}L_z-\frac{16}{3}L_z^2-\frac{107}{18}\right)\frac{1}{z^3}\\
&\quad+\left(\frac{2}{9}L_z-\frac{1}{3}L_z^2+\frac{263}{288}\right)\frac{1}{z^4}\\
&\quad+\left(\frac{47}{225}L_z-\frac{2}{15}L_z^2+\frac{3521}{18000}\right)\frac{1}{z^5}\\
&\quad+\left(\frac{26}{225}L_z-\frac{1}{15}L_z^2+\frac{10243}{108000}\right)\frac{1}{z^6} \qquad (37)\\
&\quad\left.+\left(\frac{743}{11025}L_z-\frac{4}{105}L_z^2+\frac{532267}{9261000}\right)\frac{1}{z^7}\right]+\ldots,
\end{aligned}$$

with $L_z = -(\ln(-z))/2$.

In order to incorporate the available information at threshold one has to perform an analytical continuation of

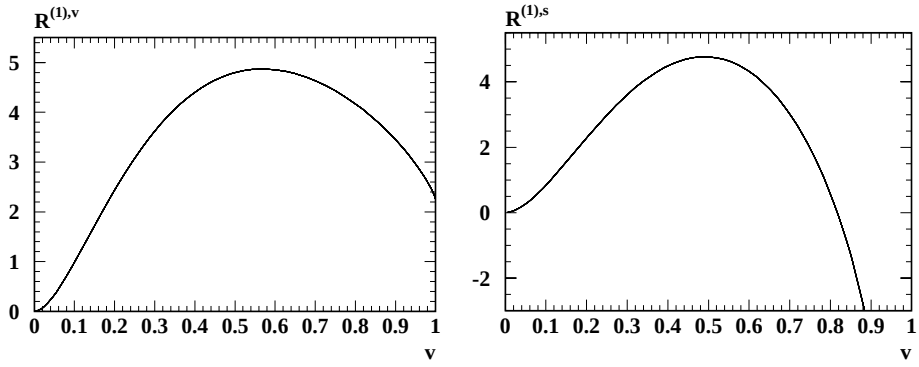

Fig. 2. $R^{(1),v}(s)$ and $R^{(1),s}(s)$ as a function of v

the expressions in (30) and (31). Taking the logarithmic parts of (30) and (31) one obtains the quadratic and cubic logarithms for the polarization functions which read

$$\begin{aligned}
\Pi^{(1),v,\mathrm{thr}}_{\log} &= \frac{3}{16\pi^2}\frac{3}{2}\left(1-\frac{1}{z}\right)^2 \ln^2\frac{1}{1-z},\\
\Pi^{(2),v,\mathrm{thr}}_{FF,\log} &= \frac{3}{16\pi^2}\left(1-\frac{1}{z}\right)^2\\
&\quad\times\left[\left(\frac{49}{16}+5\zeta_2\right)\ln^2\frac{1}{1-z}+\frac{3}{4}\ln^3\frac{1}{1-z}\right],\\
\Pi^{(2),v,\mathrm{thr}}_{FA,\log} &= \frac{3}{16\pi^2}\left(1-\frac{1}{z}\right)^2\\
&\quad\times\left[\left(\frac{423}{48}+\frac{19}{6}\zeta_2+\frac{11}{8}\ln\frac{\mu^2}{M^2}\right)\ln^2\frac{1}{1-z}\right.\\
&\quad\left.+\frac{11}{12}\ln^3\frac{1}{1-z}\right],\\
\Pi^{(2),v,\mathrm{thr}}_{FL,\log} &= \frac{3}{16\pi^2}\left(1-\frac{1}{z}\right)^2\\
&\quad\times\left[\left(-\frac{13}{4}-\frac{1}{2}\ln\frac{\mu^2}{M^2}-\frac{4}{3}\zeta_2\right)\ln^2\frac{1}{1-z}\right.\\
&\quad\left.-\frac{1}{3}\ln^3\frac{1}{1-z}\right],\\
\Pi^{(2),v,\mathrm{thr}}_{FH,\log} &= 0,\\
\Pi^{(1),s,\mathrm{thr}}_{\log} &= \frac{3}{16\pi^2}\frac{3}{2}\left(1-\frac{1}{z}\right)^2 \ln^2\frac{1}{1-z},\\
\Pi^{(2),s,\mathrm{thr}}_{FF,\log} &= \frac{3}{16\pi^2}\left(1-\frac{1}{z}\right)^2\\
&\quad\times\left[\left(\frac{73}{16}+5\zeta_2\right)\ln^2\frac{1}{1-z}+\frac{3}{4}\ln^3\frac{1}{1-z}\right],\\
\Pi^{(2),s,\mathrm{thr}}_{FA,\log} &= \frac{3}{16\pi^2}\left(1-\frac{1}{z}\right)^2\\
&\quad\times\left[\left(\frac{423}{48}+\frac{19}{6}\zeta_2+\frac{11}{8}\ln\frac{\mu^2}{M^2}\right)\ln^2\frac{1}{1-z}\right.\\
&\quad\left.+\frac{11}{12}\ln^3\frac{1}{1-z}\right],\\
\Pi^{(2),s,\mathrm{thr}}_{FL,\log} &= \frac{3}{16\pi^2}\left(1-\frac{1}{z}\right)^2\\
&\quad\times\left[\left(-\frac{13}{4}-\frac{1}{2}\ln\frac{\mu^2}{M^2}-\frac{4}{3}\zeta_2\right)\ln^2\frac{1}{1-z}\right.\\
&\quad\left.-\frac{1}{3}\ln^3\frac{1}{1-z}\right],\\
\Pi^{(2),s,\mathrm{thr}}_{FH,\log} &= 0. \qquad (38)
\end{aligned}$$

Note that, except for the coefficient of the quadratic logarithm in the structure FF, there is agreement between the coefficients of the vector and scalar correlator. The subscript "*log*" reminds one that the imaginary parts of the expressions in (38) only reproduce the logarithmic parts of (30) and (31). We want to mention that the polarization function itself also contains linear logarithmic terms which are not yet known at order α_s^2. Below we will derive numerical estimates for them. For the two-loop correlators the linear logarithms are known. They can be obtained from the constant contributions in (30) and (31).

Now the complete input is available and the individual steps described in Sect. 2 can be performed leading to a large variety of Padé approximants. For the results we present in the following those Padé approximants are chosen which contain for their construction at least terms of order z^5 and $1/z^5$ in the small and large momentum region, respectively. Furthermore we demand that the difference of the degree in the numerator and denominator in (14) is less or equal to two.

In Figs. 2 and 3 the two-loop results are plotted as a function of v and x, respectively. In addition to the roughly 15 Padé results also the exact expression is plotted. However, it is not possible to detect any difference – even close to the threshold at $v = 0$. The dashed lines in Fig. 3 correspond to the results of the high energy expansion including terms up to order $1/z^7$. Although in these curves only the information from $x \to 0$ is incorporated one observes a perfect agreement with the exact results up to $x \approx 0.9$ ($v \approx 0.10$).

The Padé results for the individual color structures at order α_s^2 are plotted in Figs. 4, 5, 6 and 7. Again, despite the fact that in each plot approximately 15 curves are shown no difference between them can be observed. In those plots where x is chosen for the abscissa also the result of the high energy expansion containing terms up to order $1/z^7$ is plotted as a dashed line. There is excellent agreement with the semi-numerical result at least up to $x \approx 0.5$, which corresponds to $v \approx 0.60$. In some cases even

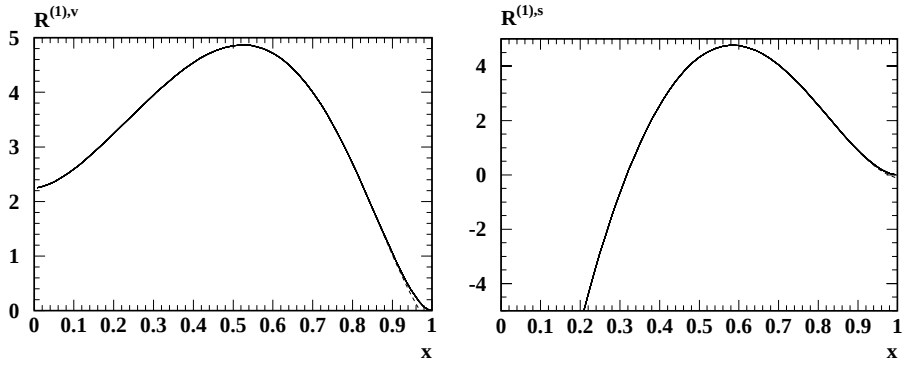

Fig. 3. $R^{(1),v}(s)$ and $R^{(1),s}(s)$ as a function of x

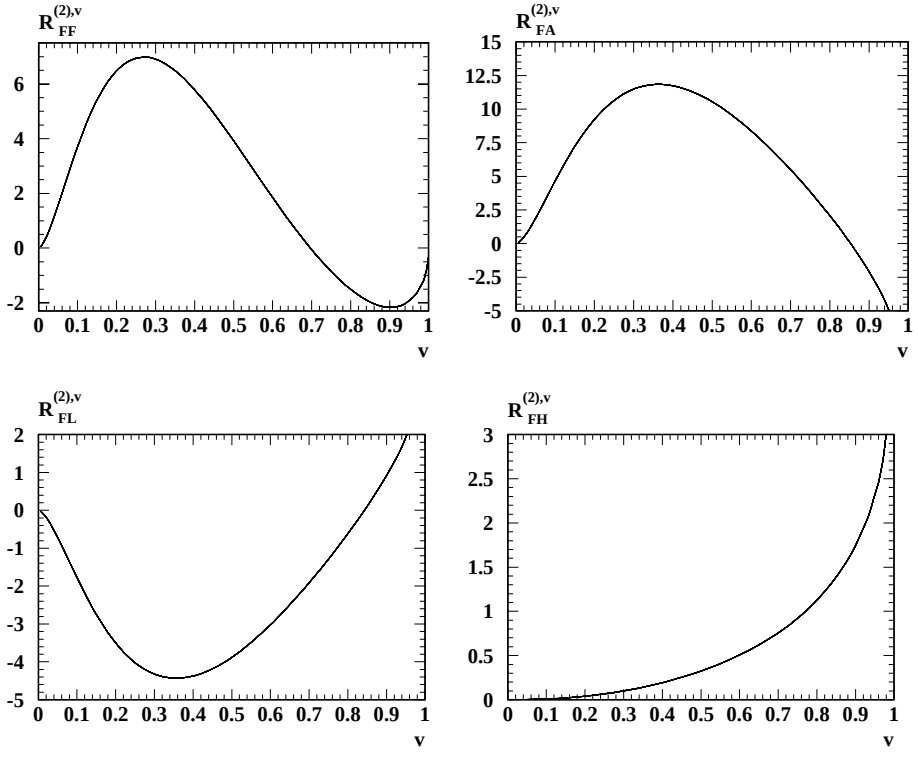

Fig. 4. $R_{FF}^{(2),v}(s)$, $R_{FA}^{(2),v}(s)$, $R_{FL}^{(2),v}(s)$ and $R_{FH}^{(2),v}(s)$ as a function of v

an agreement up to $x \approx 0.7$ is observed. This corresponds to $v \approx 0.34$ which is already quite close to the threshold.

A remark concerning the plots for $R_{FA}^{(2),s}$ and $R_{\rm L}^{(2),s}$ are in order. In Fig. 7 it can be seen that for $x \to 0$ they tend to $+\infty$ and $-\infty$, respectively. However, the turn-over takes place in a small region of x which is beyond the resolution in Fig. 6 where the variable v is used and thus the high energy region, i.e. the region for $v \to 1$, gets squeezed.

The analytical formulae which result from the semi-numerical Padé procedure are quite long. Thus we refrain from listing them explicitly. Instead, a typical representative for the two-loop results and for each color structure at three-loops can be found under the URL http://www-ttp.physik.uni-karlsruhe.de/Progdata/ttp00/ttp00-25.

5 Spectral function in HQET

In this section we concentrate on the behavior close to the threshold. In particular we want to extract the leading non-logarithmic term which is of order v^2 and afterwards transform the result to HQET.

The expressions in (38) are constructed in such a way that the combination $\mathrm{Im}[\Pi(q^2) - \Pi_{\log}^{\rm thr}(q^2)]/v^2$ approaches a constant for $v \to 0$. However, in the method we use for the computation of $\Pi(q^2)$ it is not possible to incorporate the constraint that $\mathrm{Im}[\Pi(q^2)] \sim v^2$ in analytical form. Our procedure provides rather a function which numerically imitates the quadratic dependence. As a consequence the expression $\mathrm{Im}[\Pi(q^2) - \Pi_{\log}^{\rm thr}(q^2)]/v^2$ diverges for very small velocities and provides quite different numerical values for the different Padé approximants. Nevertheless one could try to extract numerical approximations for the non-logarithmic coefficient.

For this aim we consider the quantity

$$\begin{aligned} T_X^{(i),\delta}(v) &= [n_\delta \mathrm{Im}[\Pi_X^{(i),\delta}(s + \mathrm{i}\epsilon)] \\ &\quad - R_{X,\log}^{(i),\delta,\rm thr}(s)]|_{s=M^2(1+v)/(1-v)} \\ &= N_c c_X^\delta v^2 + \mathcal{O}(v^3), \end{aligned} \tag{39}$$

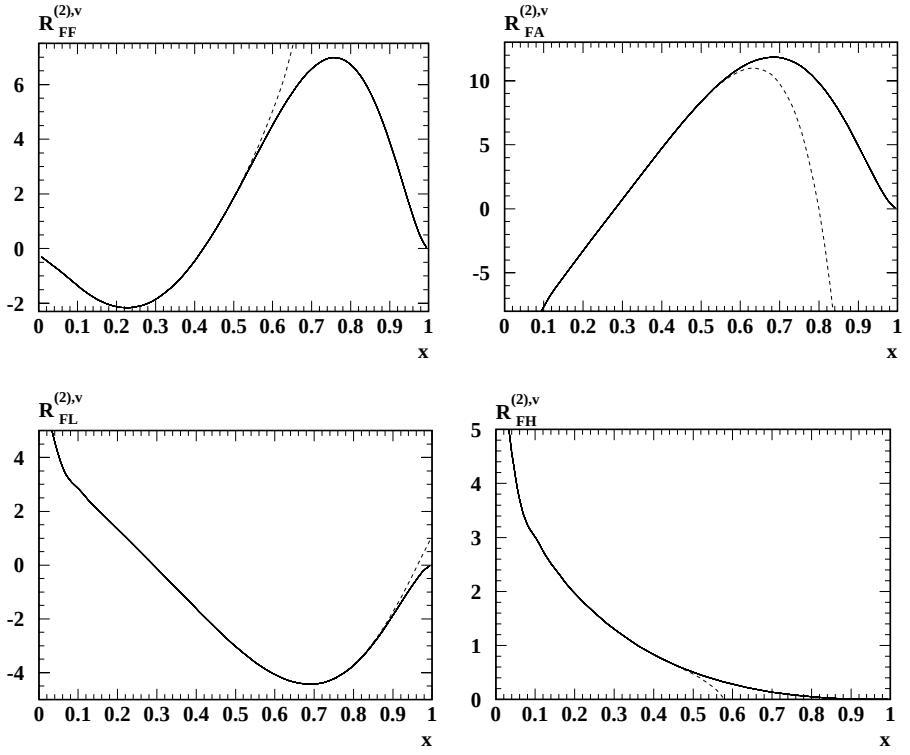

Fig. 5. $R_{FF}^{(2),v}(s)$, $R_{FA}^{(2),v}(s)$, $R_{FL}^{(2),v}(s)$ and $R_{FF}^{(2),v}(s)$ as a function of x

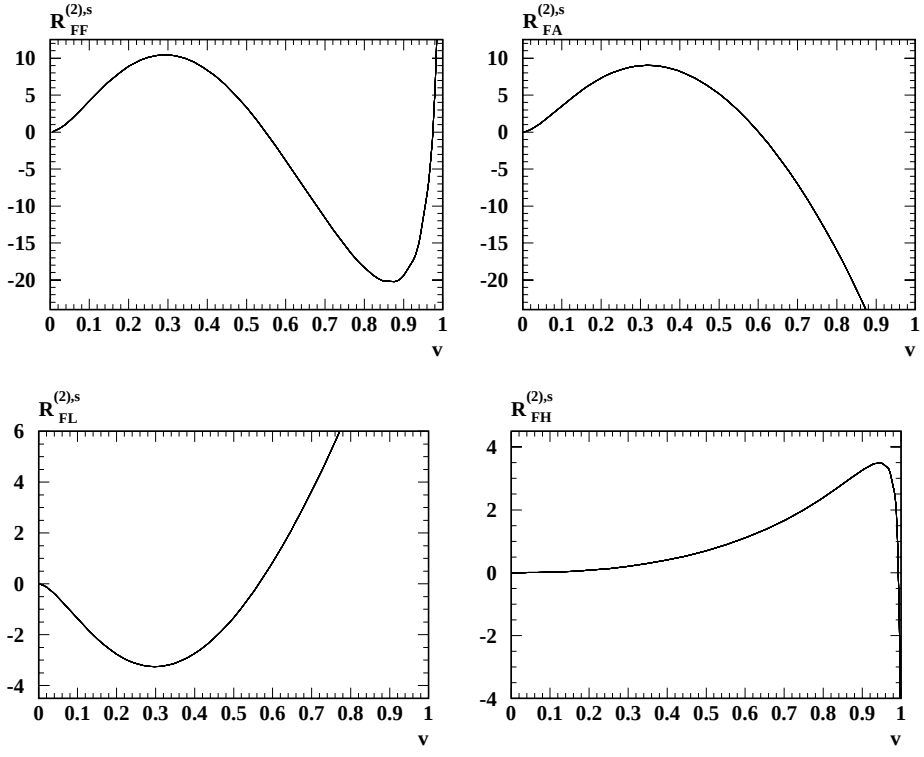

Fig. 6. $R_{FF}^{(2),s}(s)$, $R_{FA}^{(2),s}(s)$, $R_{FL}^{(2),s}(s)$ and $R_{FH}^{(2),s}(s)$ as a function of v

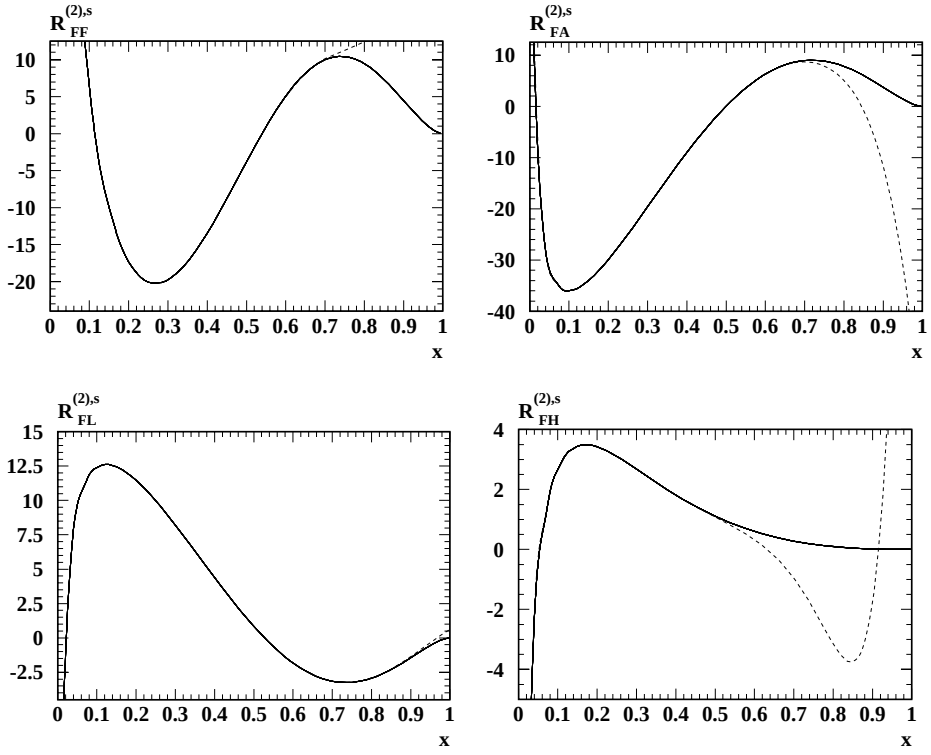

Fig. 7. $R_{FF}^{(2),s}(s)$, $R_{FA}^{(2),s}(s)$, $R_{FL}^{(2),s}(s)$ and $R_{FH}^{(2),s}(s)$ as a function of x

where $n_v = 12\pi$, $n_s = 8\pi$ and $X \in \{F, FF, FA, FL, FH\}$. $R_{X,\log}^{(i),\delta,\mathrm{thr}}$ is obtained from (30) and (31) by setting the unknown constants c_X^δ to zero. We want to use $T_X^{(i),\delta}(v)$ in order to fit the coefficient c_X^δ in (39) for each individual Padé approximant. This requires small values of v. However, due the very structure of the Padé result the ratio $T_X^{(i),\delta}(v)/v^2$ becomes unstable for $v \to 0$. Thus, in a first step we determine a minimal value v_0 for which $T_X^{(i),\delta}(v)/v^2$ evaluated for all Padé results still show reasonable agreement. Furthermore we determine an effective coefficient from the equation

$$T_X^{(i),\delta}(v_0) = N_c c_{X,\mathrm{eff}}^\delta v_0^2, \tag{40}$$

and require that the error on $c_{X,\mathrm{eff}}^\delta$ from the different Padé approximants is less than 10%. The results for v_0 and $c_{X,\mathrm{eff}}^\delta$ for each color factor both for the vector and scalar current can be found in Table 1.

In order to account also for higher order terms we choose in a next step a value $v_1 > v_0$ in such a way that, first, $v_1 - v_0 \approx v_0$ and, second, $T_X^{(i),\delta}(v)/v^2$ displays an approximately linear behavior for $v_0 \le v \le v_1$. Then a two-parametric fit is performed in the interval $[v_0, v_1]$, i.e. the coefficients c_X^δ and d_X^δ are determined from the equation

$$T_X^{(i),\delta}(v) = N_c v^2 (c_X^\delta + d_X^\delta v). \tag{41}$$

Finally (32) and (33) are used to convert the result for c_X^δ to a numerical estimate for $\tilde{c}_X$. The corresponding results for the individual structures can again be found in Table 1.

Table 1. Results from the fits for the coefficients as described in the text separated according to the color factors and the tensorial structure of the current correlator. The errors indicated in the brackets arise from the comparison of the different Padé approximants. They are omitted in the case of $\tilde{c}_X$ as they are much smaller than the systematic error of the extraction procedure

X	δ	v_0	$c_{X,\mathrm{eff}}^\delta$	v_1	c_X^δ	d_X^δ	$\tilde{c}_X$
F	v	0.01	24.4(0.1)	0.02	26.3(0.2)	−203.(9.)	6.4
F	s	0.01	20.9(0.1)	0.02	21.8(0.1)	−97.(7.)	6.5
FF	v	0.03	−9.8(0.9)	0.05	12.1(1.8)	−755.(41.)	17.4
FF	s	0.02	47.9(1.9)	0.04	58.8(2.9)	−567.(70.)	20.7
FA	v	0.03	−30.5(0.5)	0.06	−18.2(1.0)	−459.(14.)	1.2
FA	s	0.045	−11.6(0.4)	0.09	−3.4(0.6)	−201.(7.)	1.3
FL	v	0.01	5.6(0.1)	0.02	2.0(0.2)	380.(11.)	−2.0
FL	s	0.01	−1.9(0.1)	0.02	−3.8(0.1)	202.(6.)	−2.3

The corresponding errors are omitted in the case of $\tilde{c}_X$ since they are much smaller than the systematic error of the extraction procedure.

In order to get confidence in our prescription for the determination of c_X^δ let us have a look at the two-loop results. The values given in Table 1 can be compared with the exact results which read

$$\begin{aligned} c_F^v &= 27.00, \\ c_F^s &= 22.00, \\ \tilde{c}_F &= 6.50. \end{aligned} \tag{42}$$

One observes a very good agreement of the approximated results for both $\tilde{c}_F$ and c_F^δ with the exact ones[2]. Although the error induced by the comparison of the different Padé approximations is slightly smaller than the deviation from the exact result the considerations at order α_s are quite promising for the determination of the coefficients at order α_s^2.

As was already mentioned above the coefficients c_{FH}^δ are completely determined. Thus, also they can be used in order to test our prescription. However, both in the vector and scalar case c_{FH}^δ is close to zero which, of course, leads to large relative errors. Nevertheless, let us present the results which read for $v_0 = 0.05$ and $v_1 = 0.1$ [3]

$$\begin{aligned} c_{FH,\text{eff}}^v &= 0.20(6), \\ c_{FH}^v &= 0.16(10), \\ c_{FH,\text{eff}}^s &= 0.50(6), \\ c_{FH}^s &= 0.44(11). \end{aligned} \tag{43}$$

The comparison with the exact values obtained from (30) and (31)

$$\begin{aligned} c_{FH}^v &= 0.175\ldots, \\ c_{FH}^s &= 0.455\ldots, \end{aligned} \tag{44}$$

shows that the agreement of the central values is within 10%.

In order to obtain our final predictions for the coefficients $\tilde{c}_X$ we proceed as follows: the coefficients $\tilde{c}_X$ given in Table 1 have to be independent from the tensorial structure of the current correlator from which they are determined. On the other hand, guided by the numbers shown in Table 1, we can define criteria concerning the stability and reliability of the extraction procedure. As a first criterion we require that v_0 should be as small as possible. This clearly suppresses higher order terms in v. Furthermore we consider the ratio d_X^δ/c_X^δ and regard that color structure as more reliable where the ratio is smallest. As d_X^δ represents an effective constant containing the effects of the higher orders in v also this criterion selects the structure where they are suppressed as compared to the v^2 terms. Following these rules we choose the vector correlator in order to obtain $\tilde{c}_{FA}$ and the scalar one for $\tilde{c}_{FF}$ and $\tilde{c}_{FL}$. This leads to the following results

$$\begin{aligned} \tilde{c}_{FF} &= 21(6), \\ \tilde{c}_{FA} &= 1.2(4), \\ \tilde{c}_{FL} &= -2.3(7), \end{aligned} \tag{45}$$

where we assigned a conservative error of 30%. Note that all numbers given in the last column of Table 1 are consistent with our final predictions of (45).

In practical applications it is often sufficient to know the result at order α_s^2 for the numerical value $N_c = 3$ which motivates the following procedure: in a first step the moments of the color structures FF, FA and FL are added for fixed n_l and the Padé procedure is performed. Afterwards the prescription described around (39) is applied. The results of the corresponding analysis can be found in Table 2 which allow one to deduce the following compact expression for $\tilde{c}_{n_l}$ which governs the dependence on n_l:

$$\tilde{c}_{n_l} = 46(15) - 1.2(4) n_l. \tag{46}$$

At first sight the errors appear quite large. However, one has to recall that only the large- and small-q^2 behavior of the polarization function serves as input whereas the quantity in (46) corresponds to the imaginary part at $q^2 = M^2$. Note also that at order α_s^2 the numerical values for v_0 have to be chosen larger than at order α_s which increases the influence of the higher order terms in v.

To summarize: the complicated threshold structure of the Padé approximants allows only a rather rough determination of the constants c^v and c^s. However, the peculiar structure of (32) and (33) connecting c^δ to $\tilde{c}$ makes it possible to extract the universal coefficient $\tilde{c}$ with a reasonable accuracy.

Finally we are in the position to write down the expression for $\tilde{R}'(\omega)$ up to order α_s^2. Inserting the color factors into (29) and using the results from (46) one obtains

$$\begin{aligned} \tilde{R}'(\omega) = N_c \omega^2 \Bigg[1 + \frac{\alpha_s^{(n_l)}(\mu)}{\pi}(8.667 + L_\omega) + \left(\frac{\alpha_s^{(n_l)}(\mu)}{\pi}\right)^2 \\ \times \Big(46(15) + 35.54 L_\omega + 1.875 L_\omega^2 \\ + n_l(-1.2(4) - 1.583 L_\omega - 0.08333 L_\omega^2) \Big) \Bigg]. \end{aligned} \tag{47}$$

We can conclude that the coefficient at order α_s^2 is quite large and has a mild dependence on n_l.

Table 2. Results from the fits for the coefficients as described in the text separated for different values of n_l. As far as the errors are concerned the same statements hold as in Table 1

n_l	δ	v_0	$c_{n_l,\text{eff}}^\delta$	v_1	$c_{n_l}^\delta$	$d_{n_l}^\delta$	$\tilde{c}_{n_l}$
0	v	0.03	−143.0(3.7)	0.05	−46.9(7.5)	−3324.(142.)	36.5
0	s	0.03	46.3(2.1)	0.05	106.8(4.4)	−2069.(92.)	46.2
1	v	0.03	−134.7(3.5)	0.05	−42.5(7.1)	−3189.(136.)	35.7
1	s	0.03	47.5(2.1)	0.05	105.6(4.3)	−1984.(90.)	45.0
2	v	0.03	−126.4(3.3)	0.05	−38.1(6.7)	−3055.(129.)	34.8
2	s	0.03	48.8(2.0)	0.05	104.4(4.2)	−1898.(88.)	43.9
3	v	0.03	−118.0(3.1)	0.05	−33.6(6.3)	−2921.(121.)	34.0
3	s	0.03	50.1(1.9)	0.05	103.2(4.1)	−1814.(84.)	42.7
4	v	0.03	−109.6(2.7)	0.05	−28.9(5.6)	−2793.(108.)	33.2
4	s	0.03	51.4(1.9)	0.05	102.0(3.9)	−1728.(81.)	41.5
5	v	0.03	−101.4(2.7)	0.05	−24.8(5.5)	−2651.(108.)	32.3
5	s	0.03	52.6(1.8)	0.05	100.7(3.8)	−1642.(79.)	40.3

[2] This is also the case for $v_0 = 0.03$ and $v_1 = 0.06$

[3] As can be seen in Figs. 4 and 6 both $R_{FH}^{(2),v}$ and $R_{FH}^{(2),s}$ are rather smooth around $v = 0$ which allows for larger values of v_0 and v_1

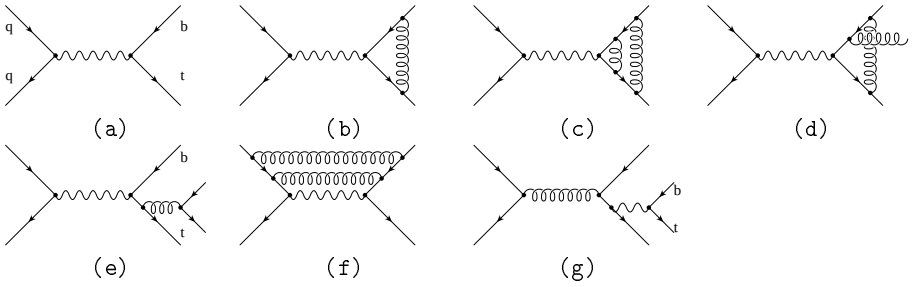

Fig. 8a–g. Sample diagrams contributing to the process $q\bar{q} \to t\bar{b}$. The wavy and loopy lines represent W bosons and gluons, respectively

6 Applications and conclusions

As an application of the vector and axial-vector current correlator we want to discuss the single-top-quark production via the process $q\bar{q} \to t\bar{b}$. Some sample diagrams contributing to this process are shown in Fig. 8.

The corrections of order α_s to the (total) single-top-quark production rate are quite large. They amount to about 54% and 50% for Tevatron and LHC energies, respectively [25], where 18%, respectively, 17% arise from the final state corrections. This makes it necessary to consider also the corrections of order α_s^2. Due to the appearance of an interference between the initial and final state (cf. Figure 8f), which for the first time happens at order α_s^2, the complete calculation is a non-trivial task. However, with the results of this paper we are in the position to perform a first step and consider the leading term in the large-N_c expansion.

One observes that the contributions of the diagrams where gluons connect the initial and final states are suppressed by at least a factor $1/N_c^2$ in the large N_c limit as compared to the diagrams in Figs. 8c–e. For the latter, together with the contributions of Figs. 8a,b, the differential cross section can be written in factorized form

$$\frac{\mathrm{d}\sigma}{\mathrm{d}q^2}(p\bar{p} \to t\bar{b} + X) = \sigma(p\bar{p} \to W^* + X) \frac{\mathrm{Im}\Pi_W(q^2, M_t^2, M_b^2)}{\pi(q^2 - M_W^2)^2}, \quad (48)$$

where Π_W corresponds to the transversal part of the W boson self energy which is connected to the vector correlator of (1) through

$$\Pi_W(q^2) = \sqrt{2} G_\mathrm{F} M_W^2 |V_{tb}|^2 q^2 \Pi^v(q^2). \quad (49)$$

At order α_s^2 there are also diagrams like the one in Fig. 8g which appear for the first time. In principle they also lead to the same final state as the diagram in Fig. 8e. However, one has to note that the W boson generating the top and bottom quark is radiated from a light quark flavor. This suggests that their contribution is small although there is only a suppression by a factor $1/N_c$ as compared to Fig. 8c and not by $1/N_c^2$ like for the diagram in Fig. 8f.

Thus, if we restrict ourselves to the leading term in $1/N_c$ it is possible to use the results for R^v obtained above in combination with (48) to perform a theoretical analysis at order α_s^2 to the single-top-quark production in the large-N_c limit. In order to obtain the total cross section the corresponding parton distribution functions would be needed to the same order.

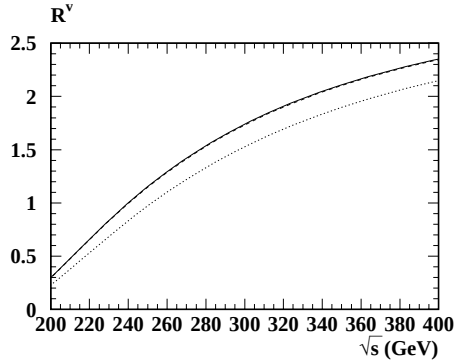

Fig. 9. LO (dotted), NLO (dashed) and NNLO (solid) results of $R^v(s)$

The production cross section of the virtual W^* boson is identical to that of the Drell–Yan process $q\bar{q} \to e\bar{\nu}_e$. The latter is known to $\mathcal{O}(\alpha_s^2)$ from [26]. Thus we can take the proper ratios to make predictions in the large-N_c limit at NNLO free from any dependence on parton distribution functions. As an example, we can consider the following expression

$$\frac{\frac{\mathrm{d}\sigma}{\mathrm{d}q^2}(pp \to W^* \to tb)}{\frac{\mathrm{d}\sigma}{\mathrm{d}q^2}(pp \to W^* \to e\nu_e)} = \frac{\mathrm{Im}[\Pi_{tb}(q^2)]}{\mathrm{Im}[\Pi_{e\nu}(q^2)]} = N_c |V_{tb}|^2 R^v(s). \quad (50)$$

In Fig. 9 the LO, NLO and NNLO results of $R^v(s)$ are plotted in the range $s^{1/2} = 200 \ldots 400\,\mathrm{GeV}$ where $M_t = 175\,\mathrm{GeV}$ and $\alpha_s(M_Z) = 0.118$ has been chosen for the numerical analysis. Whereas the $\mathcal{O}(\alpha_s)$ corrections are significant there is only a moderate contribution from the order α_s^2 terms. In the range in q^2 shown in Fig. 9 they are below 1% of the Born result. Note that the NNLO correction to the Drell–Yan process are also small and amount to at most a few percent (see e.g. [27]). Thus, in case there is no kinematical magnification for the diagrams in Figs. 8f,g we can conclude that the radiative corrections to the single-top-quark production via the process $q\bar{q} \to t\bar{b}$ are well under control.

The scalar and pseudo-scalar correlator covers properties connected to a charged Higgs boson. The latter appear in theories beyond the SM which are usually characterized

by an enlarged Higgs sector containing Higgs bosons with different quantum numbers. For example, one of the most appealing extensions of the SM, the minimal supersymmetric standard model (MSSM), contains two complex iso-doublets with opposite hyper-charge (see e.g. [28]), resulting in five mass eigenstates of (pseudo-)scalar physical Higgs fields: two neutral CP even (H^0 and h^0), one neutral CP odd (A) and two charged ($H^\pm$) Higgs bosons.

Let us consider a generic charged Higgs boson coupled to fermions through

$$\mathcal{L}_{H^+D\bar{U}} = (\sqrt{2}G_{\rm F})^{1/2} H^+ J_{H^+}, \tag{51}$$

where the corresponding quark current is given by

$$J_{H^+} = \frac{m_U}{\sqrt{2}} \bar{U}[a(1-\gamma_5) + b(1+\gamma_5)]D. \tag{52}$$

Here U and D represent generic up- and down-type quarks, respectively, with $\overline{\rm MS}$ masses m_U and $m_D = 0$. Equation (52) only covers the contributions from a H^+ boson; the formulae for a Higgs boson with negative charge are analogous. The parameters a and b are model dependent and are left unspecified.

The decay rate of the boson H^+ into quarks and gluons can be written in the form

$$\Gamma(H^+ \to U\bar{D}) = \sqrt{2} G_{\rm F} M_{H^+} {\rm Im}[\Pi_H(M_{H^+}^2)], \tag{53}$$

where M_U is the pole quark mass and $\Pi_H(q^2)$ is given by

$$\begin{aligned} q^2 \Pi_H(q^2) &= \int {\rm d}x {\rm e}^{{\rm i}qx} \langle T J_{H^-}(x) J_{H^-}(0)\rangle \\ &= (a^2+b^2) q^2 \Pi^s(q^2), \end{aligned} \tag{54}$$

Thus, we arrive at the following expression for the hadronic decay rate of the charged Higgs boson

$$\Gamma(H^+ \to U\bar{D}) = \frac{\sqrt{2}G_{\rm F}}{8\pi} M_{H^+} (a^2+b^2) R^s(M_{H^+}^2). \tag{55}$$

In Fig. 10 $R^s(M_{H^+}^2)$ is plotted at LO, NLO and NNLO. Again it turns out that the radiative corrections are well under control as order α_s^2 terms contribute at most of the order of 1%.

As an application of the correlator in the effective theory we want to mention the determination of the meson decay constants via QCD sum rules where the Borel transform of $\tilde{R}'$ as given in (47) enters as a building block. Besides the perturbative part the sum rules also obtain contributions from non-perturbative condensates which, however, are numerical less important [4]. The typical scale which has to be used in (47) is of the order of 1 GeV [4,5] which leads to sizeable corrections both at order α_s and at order α_s^2.

To be more precise let us choose $\alpha_s^{(5)}(M_Z) = 0.118$ which, using two-loop accuracy, leads to $\alpha_s^{(4)}(1.3\,{\rm GeV}) \approx 0.37$ [29]. For $\omega = 1.3\,{\rm GeV}$ and $n_l = 4$ the order α_s corrections in (47) amount to about 100%. The terms at $\mathcal{O}(\alpha_s^2)$ contribute with additional 60(20)% where the sign is the same as for the LO correction. A careful analysis is necessary in order to decide whether perturbation theory can safely be applied in this case.

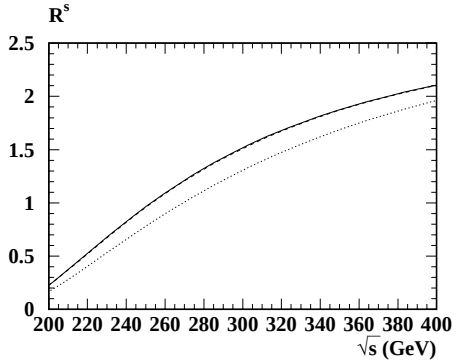

Fig. 10. LO (dotted), NLO (dashed) and NNLO (solid) results of $R^s(s)$, $M = M_t = 175\,{\rm GeV}$

To conclude, in this paper the non-diagonal current correlator formed by a massive and massless quark has been considered. Moments in the low and high energy region have been computed analytically in full QCD. Furthermore the leading logarithmic contributions arising at the quark threshold $q^2 = M^2$ have been obtained from the reconstruction of the logarithmic terms of the spectral function in the effective theory. This information is combined with the help of conformal mapping and Padé approximation to obtain semi-numerical results for the vector and scalar correlator and in particular their imaginary parts valid for all values of q and M. In a next step the various Padé results are used in order to obtain the leading non-logarithmic coefficient at threshold which is in turn transformed to the effective theory leading to a prediction of the spectral function up to order α_s^2 (see (47)). As applications we considered the effect of the α_s^2 correction to the single-top-quark production and the decay of a charged Higgs boson.

Acknowledgements. The authors are grateful to A. Grozin, J.H. Kühn and V.A. Smirnov for useful discussions and advice. This work was supported in part by the DFG-Forschergruppe "Quantenfeldtheorie, Computeralgebra und Monte-Carlo-Simulation" (contract FOR 264/2-1), by SUN Microsystems through Academic Equipment Grant No. 14WU0148 and by the European Union under contract HPNN-CT-2000-00149.

Appendix: Analytical results for the moments at order α_s^2

In the limit $z \to 0$ the results for $\Pi^{(2),v}$ and $\Pi^{(2),s}$ parameterized in terms of the on-shell mass read

$$\begin{aligned} \Pi_{FF}^{(2),v} = \frac{3}{16\pi^2} \Bigg[&+ \left(- \left(\frac{245}{48} \frac{1}{\sqrt{3}} C_l \right) + \frac{3}{2} C_l^2 \right. \\ &\left. + \left(-3\ln 2 + \frac{80579}{25920} \right) \zeta_2 + \frac{179}{144} \zeta_3 - \frac{5}{16} \zeta_4 \right. \end{aligned}$$

$$
\begin{aligned}
&+\frac{649}{41472}\Big)z+\Big(-\Big(\frac{6187}{1800}\frac{1}{\sqrt{3}}C_l\Big)+\frac{2}{5}C_l^2\\
&+\Big(-\Big(\frac{8}{5}\ln 2\Big)+\frac{54089}{40500}\Big)\zeta_2+\frac{4261}{2700}\zeta_3\\
&-\frac{1}{12}\zeta_4+\frac{15229}{51840}\Big)z^2\\
&+\Big(-\Big(\frac{26869}{364500}\frac{1}{\sqrt{3}}C_l\Big)+\frac{1}{6}C_l^2\\
&+\Big(-\ln 2+\frac{1637813}{2268000}\Big)\zeta_2+\frac{409}{2700}\zeta_3-\frac{5}{144}\zeta_4\\
&+\frac{5303639}{23328000}\Big)z^3+\Big(-\Big(\frac{31433}{79380}\frac{1}{\sqrt{3}}C_l\Big)+\frac{3}{35}C_l^2\\
&+\Big(-\Big(\frac{24}{35}\ln 2\Big)+\frac{455767}{1029000}\Big)\zeta_2+\frac{155243}{396900}\zeta_3\\
&-\frac{1}{56}\zeta_4+\frac{7315733}{65318400}\Big)z^4\\
&+\Big(\frac{552604783}{800150400}\frac{1}{\sqrt{3}}C_l+\frac{1}{20}C_l^2\\
&+\Big(-\Big(\frac{1}{2}\ln 2\Big)+\frac{523855033}{1778112000}\Big)\zeta_2-\frac{59293}{423360}\zeta_3\\
&-\frac{1}{96}\zeta_4+\frac{2245278797}{34139750400}\Big)z^5\\
&+\Big(\frac{1448186461}{5952139200}\frac{1}{\sqrt{3}}C_l+\frac{2}{63}C_l^2\\
&+\Big(-\Big(\frac{8}{21}\ln 2\Big)+\frac{82974271}{400075200}\Big)\zeta_2+\frac{26561}{317520}\zeta_3\\
&-\frac{5}{756}\zeta_4+\frac{23465474813}{1904684544000}\Big)z^6\Big]+\ldots,
\end{aligned}
$$

$$
\begin{aligned}
\Pi_{FA}^{(2),v}=\frac{3}{16\pi^2}\Big[&+\Big(\frac{245}{96}\frac{1}{\sqrt{3}}C_l-\frac{3}{4}C_l^2\\
&+\Big(\frac{3}{2}\ln 2+\frac{6757}{10368}\Big)\zeta_2-\frac{1093}{864}\zeta_3\\
&-\frac{27}{32}\zeta_4+\frac{147835}{82944}\Big)z\\
&+\Big(\frac{6187}{3600}\frac{1}{\sqrt{3}}C_l-\frac{1}{5}C_l^2+\Big(\frac{4}{5}\ln 2+\frac{66997}{324000}\Big)\zeta_2\\
&-\frac{2711}{2700}\zeta_3-\frac{9}{40}\zeta_4+\frac{112693}{129600}\Big)z^2\\
&+\Big(\frac{26869}{729000}\frac{1}{\sqrt{3}}C_l-\frac{1}{12}C_l^2+\Big(\frac{1}{2}\ln 2+\frac{4573}{54000}\Big)\zeta_2\\
&-\frac{69}{400}\zeta_3-\frac{3}{32}\zeta_4+\frac{11769743}{23328000}\Big)z^3\\
&+\Big(\frac{31433}{158760}\frac{1}{\sqrt{3}}C_l-\frac{3}{70}C_l^2\\
&+\Big(\frac{12}{35}\ln 2+\frac{144869}{3472875}\Big)\zeta_2\\
&-\frac{24547}{99225}\zeta_3-\frac{27}{560}\zeta_4+\frac{39697543}{114307200}\Big)z^4\\
&+\Big(-\Big(\frac{552604783}{1600300800}\frac{1}{\sqrt{3}}C_l\Big)-\frac{1}{40}C_l^2\\
&+\Big(\frac{1}{4}\ln 2+\frac{16650583}{711244800}\Big)\zeta_2+\frac{23603}{604800}\zeta_3\\
&-\frac{9}{320}\zeta_4+\frac{16737914551}{68279500800}\Big)z^5\\
&+\Big(-\Big(\frac{1448186461}{11904278400}\frac{1}{\sqrt{3}}C_l\Big)-\frac{1}{63}C_l^2\\
&+\Big(\frac{4}{21}\ln 2+\frac{69820073}{4800902400}\Big)\zeta_2-\frac{8417}{136080}\zeta_3\\
&-\frac{1}{56}\zeta_4+\frac{10342199087}{53331167232}\Big)z^6\Big]+\ldots,
\end{aligned}
$$

$$
\begin{aligned}
\Pi_{FL}^{(2),v}=\frac{3}{16\pi^2}\Big[&+\Big(-\Big(\frac{125}{216}\zeta_2\Big)+\frac{1}{3}\zeta_3-\frac{871}{1728}\Big)z\\
&+\Big(-\Big(\frac{367}{1350}\zeta_2\Big)+\frac{4}{45}\zeta_3-\frac{1373}{6480}\Big)z^2\\
&+\Big(-\Big(\frac{11}{72}\zeta_2\Big)+\frac{1}{27}\zeta_3-\frac{25771}{233280}\Big)z^3\\
&+\Big(-\Big(\frac{12857}{132300}\zeta_2\Big)+\frac{2}{105}\zeta_3-\frac{43117}{680400}\Big)z^4\\
&+\Big(-\Big(\frac{10133}{151200}\zeta_2\Big)+\frac{1}{90}\zeta_3-\frac{112051}{2903040}\Big)z^5\\
&+\Big(-\Big(\frac{34933}{714420}\zeta_2\Big)+\frac{4}{567}\zeta_3-\frac{718927}{29393280}\Big)z^6\Big]\\
&+\ldots,
\end{aligned}
$$

$$
\begin{aligned}
\Pi_{FH}^{(2),v}=\frac{3}{16\pi^2}\Big[&+\Big(\frac{139}{12}\frac{1}{\sqrt{3}}C_l+\zeta_2-\frac{194}{27}\zeta_3+\frac{665}{1728}\Big)z\\
&+\Big(\frac{382}{25}\frac{1}{\sqrt{3}}C_l+\frac{8}{15}\zeta_2-\frac{1168}{135}\zeta_3+\frac{9661}{16200}\Big)z^2\\
&+\Big(\frac{1400461}{72900}\frac{1}{\sqrt{3}}C_l+\frac{1}{3}\zeta_2-\frac{4102}{405}\zeta_3\\
&+\frac{440741}{1166400}\Big)z^3+\Big(\frac{13738391}{595350}\frac{1}{\sqrt{3}}C_l+\frac{8}{35}\zeta_2\\
&-\frac{3644}{315}\zeta_3+\frac{52709}{4762800}\Big)z^4\\
&+\Big(\frac{128030963}{4762800}\frac{1}{\sqrt{3}}C_l+\frac{1}{6}\zeta_2-\frac{1363}{105}\zeta_3\\
&-\frac{8545133}{20321280}\Big)z^5+\Big(\frac{15959744567}{520812180}\frac{1}{\sqrt{3}}C_l\\
&+\frac{8}{63}\zeta_2-\frac{24452}{1701}\zeta_3-\frac{147478621319}{166659897600}\Big)z^6\Big]+\ldots,
\end{aligned}
$$

$$
\begin{aligned}
\Pi_{FF}^{(2),s}=\frac{3}{16\pi^2}\Big[&+\Big(\frac{7}{2}\sqrt{3}C_l+2C_l^2+\frac{121}{144}\zeta_2-\frac{85}{12}\zeta_3\\
&-\frac{5}{12}\zeta_4+\frac{103}{384}\Big)z+\Big(-\Big(\frac{283}{80}\sqrt{3}C_l\Big)+\frac{1}{2}C_l^2\\
&+\Big(-\ln 2+\frac{59623}{43200}\Big)\zeta_2
\end{aligned}
$$

$$
\begin{aligned}
&+\frac{3461}{720}\zeta_3-\frac{5}{48}\zeta_4+\frac{23477}{69120}\Big)z^2\\
&+\Big(\frac{1049}{1800}\frac{1}{\sqrt{3}}C_l+\frac{1}{5}C_l^2\\
&+\Big(-\Big(\frac{4}{5}\ln 2\Big)+\frac{92717}{108000}\Big)\zeta_2-\frac{923}{1800}\zeta_3\\
&-\frac{1}{24}\zeta_4+\frac{65329}{103680}\Big)z^3\\
&+\Big(-\Big(\frac{324853}{85050}\frac{1}{\sqrt{3}}C_l\Big)+\frac{1}{10}C_l^2\\
&+\Big(-\Big(\frac{3}{5}\ln 2\Big)+\frac{2892733}{5292000}\Big)\zeta_2+\frac{967}{525}\zeta_3\\
&-\frac{1}{48}\zeta_4+\frac{4524487}{10886400}\Big)z^4\\
&+\Big(\frac{442717}{1587600}\frac{1}{\sqrt{3}}C_l+\frac{2}{35}C_l^2\\
&+\Big(-\Big(\frac{16}{35}\ln 2\Big)+\frac{27193603}{74088000}\Big)\zeta_2\\
&-\frac{599}{3528}\zeta_3-\frac{1}{84}\zeta_4+\frac{33815837}{87091200}\Big)z^5\\
&+\Big(-\Big(\frac{219606437}{114307200}\frac{1}{\sqrt{3}}C_l\Big)+\frac{1}{28}C_l^2\\
&+\Big(-\Big(\frac{5}{14}\ln 2\Big)+\frac{91843391}{355622400}\Big)\zeta_2+\frac{137203}{141120}\zeta_3\\
&-\frac{5}{672}\zeta_4+\frac{3685964659}{14631321600}\Big)z^6\\
&+\Big(\frac{2861558023}{13888324800}\frac{1}{\sqrt{3}}C_l+\frac{1}{42}C_l^2\\
&+\Big(-\Big(\frac{2}{7}\ln 2\Big)+\frac{100704841}{533433600}\Big)\zeta_2-\frac{18371}{211680}\zeta_3\\
&-\frac{5}{1008}\zeta_4+\frac{10307800934177}{44442639360000}\Big)z^7\Big]+\ldots,
\end{aligned}
$$

$$
\begin{aligned}
\Pi_{FA}^{(2),s}=\frac{3}{16\pi^2}\Big[&+\Big(-\Big(\frac{7}{4}\sqrt{3}C_l\Big)-C_l^2+\frac{277}{216}\zeta_2+\frac{8}{3}\zeta_3\\
&-\frac{9}{8}\zeta_4+\frac{175}{1728}\Big)z\\
&+\Big(\frac{283}{160}\sqrt{3}C_l-\frac{1}{4}C_l^2+\Big(\frac{1}{2}\ln 2+\frac{1723}{5760}\Big)\zeta_2\\
&-\frac{3857}{1440}\zeta_3-\frac{9}{32}\zeta_4+\frac{953}{1024}\Big)z^2\\
&+\Big(-\Big(\frac{1049}{3600}\frac{1}{\sqrt{3}}C_l\Big)-\frac{1}{10}C_l^2\\
&+\Big(\frac{2}{5}\ln 2+\frac{1153}{12000}\Big)\zeta_2+\frac{31}{225}\zeta_3-\frac{9}{80}\zeta_4\\
&+\frac{33307}{64800}\Big)z^3+\Big(\frac{324853}{170100}\frac{1}{\sqrt{3}}C_l\\
&-\frac{1}{20}C_l^2+\Big(\frac{3}{10}\ln 2+\frac{313}{8400}\Big)\zeta_2\\
&-\frac{24761}{25200}\zeta_3-\frac{9}{160}\zeta_4+\frac{3961231}{10886400}\Big)z^4\\
&+\Big(-\Big(\frac{442717}{3175200}\frac{1}{\sqrt{3}}C_l\Big)-\frac{1}{35}C_l^2\\
&+\Big(\frac{8}{35}\ln 2+\frac{243241}{14817600}\Big)\zeta_2+\frac{359}{7350}\zeta_3\\
&-\frac{9}{280}\zeta_4+\frac{31355501}{152409600}\Big)z^5\\
&+\Big(\frac{219606437}{228614400}\frac{1}{\sqrt{3}}C_l-\frac{1}{56}C_l^2\\
&+\Big(\frac{5}{28}\ln 2+\frac{272033}{33868800}\Big)\zeta_2-\frac{143663}{282240}\zeta_3-\frac{9}{448}\zeta_4\\
&+\frac{4739201353}{29262643200}\Big)z^6\\
&+\Big(-\Big(\frac{2861558023}{27776649600}\frac{1}{\sqrt{3}}C_l\Big)-\frac{1}{84}C_l^2\\
&+\Big(\frac{1}{7}\ln 2+\frac{28543}{6531840}\Big)\zeta_2+\frac{4439}{158760}\zeta_3-\frac{3}{224}\zeta_4\\
&+\frac{108189401963}{1111065984000}\Big)z^7\Big]+\ldots,
\end{aligned}
$$

$$
\begin{aligned}
\Pi_{FL}^{(2),s}=\frac{3}{16\pi^2}\Big[&+\Big(-\Big(\frac{1}{6}\zeta_2\Big)+\frac{4}{9}\zeta_3-\frac{5}{48}\Big)z\\
&+\Big(-\Big(\frac{73}{360}\zeta_2\Big)+\frac{1}{9}\zeta_3-\frac{143}{576}\Big)z^2\\
&+\Big(-\Big(\frac{119}{900}\zeta_2\Big)+\frac{2}{45}\zeta_3-\frac{2083}{12960}\Big)z^3\\
&+\Big(-\Big(\frac{1123}{12600}\zeta_2\Big)+\frac{1}{45}\zeta_3-\frac{7759}{77760}\Big)z^4\\
&+\Big(-\Big(\frac{2791}{44100}\zeta_2\Big)+\frac{4}{315}\zeta_3-\frac{346519}{5443200}\Big)z^5\\
&+\Big(-\Big(\frac{9941}{211680}\zeta_2\Big)+\frac{1}{126}\zeta_3-\frac{608813}{14515200}\Big)z^6\\
&+\Big(-\Big(\frac{34387}{952560}\zeta_2\Big)+\frac{1}{189}\zeta_3-\frac{27828673}{979776000}\Big)z^7\Big]\\
&+\ldots,
\end{aligned}
$$

$$
\begin{aligned}
\Pi_{FH}^{(2),s}=\frac{3}{16\pi^2}\Big[&+\Big(7\sqrt{3}C_l-\frac{104}{9}\zeta_3+\frac{33}{16}\Big)z\\
&+\Big(\frac{479}{20}\frac{1}{\sqrt{3}}C_l+\frac{1}{3}\zeta_2-\frac{38}{3}\zeta_3+\frac{2101}{2880}\Big)z^2\\
&+\Big(\frac{12473}{450}\frac{1}{\sqrt{3}}C_l+\frac{4}{15}\zeta_2-\frac{628}{45}\zeta_3+\frac{7837}{64800}\Big)z^3\\
&+\Big(\frac{5363167}{170100}\frac{1}{\sqrt{3}}C_l+\frac{1}{5}\zeta_2-\frac{2062}{135}\zeta_3\\
&-\frac{1179673}{2721600}\Big)z^4+\Big(\frac{21024149}{595350}\frac{1}{\sqrt{3}}C_l+\frac{16}{105}\zeta_2\\
&-\frac{15688}{945}\zeta_3-\frac{37456457}{38102400}\Big)z^5
\end{aligned}
$$

$$
\begin{aligned}
&+\left(\frac{334931357}{8573040}\frac{1}{\sqrt{3}}C_l+\frac{5}{42}\zeta_2-\frac{3389}{189}\zeta_3\right.\\
&\left.-\frac{4201269473}{2743372800}\right)z^6\\
&+\left(\frac{14859593107}{347208120}\frac{1}{\sqrt{3}}C_l+\frac{2}{21}\zeta_2-\frac{10922}{567}\zeta_3\right.\\
&\left.-\frac{1154471458391}{555532992000}\right)z^7\Bigg]+\ldots,
\end{aligned}
$$

where $\mu^2=M^2$ has been adopted. In the high energy limit the corresponding results read

$$
\begin{aligned}
\Pi_{FF}^{(2),v}=&\frac{3}{16\pi^2}\left[\frac{71}{576}-\left(\frac{8}{3}C_l^2\right)+\frac{11}{2}\frac{1}{\sqrt{3}}C_l-\left(\frac{64}{3}l_4\right)\right.\\
&-\left(\frac{8}{9}\ln^4 2\right)-\left(\frac{1}{4}L_z\right)\\
&+\left(8\ln 2+\frac{16}{3}\ln^2 2-\frac{713}{216}\right)\zeta_2-\left(\frac{158}{9}\zeta_3\right)\\
&+\frac{107}{9}\zeta_4+10\zeta_5\\
&+\left(-\left(\frac{39}{4}\sqrt{3}C_l\right)-\frac{3}{2}C_l^2+32l_4+\frac{4}{3}\ln^4 2\right.\\
&+\left((15-24\ln 2)\zeta_2+15\zeta_3-\frac{121}{8}\right)L_z\\
&+\frac{15}{4}L_z^2-6L_z^3\\
&+\left(-6\ln 2-8\ln^2 2+\frac{155}{72}\right)\zeta_2+\frac{491}{12}\zeta_3\\
&\left.-\frac{363}{16}\zeta_4-\frac{85}{3}\zeta_5+\frac{3859}{288}\right)\frac{1}{z}\\
&+\left(\frac{21}{4}L_z-18L_z^2+(15-24\ln 2)\zeta_2\right.\\
&\left.+\frac{68}{3}\zeta_3-\frac{80}{3}\zeta_5-\frac{31}{24}\right)\frac{1}{z^2}\\
&+\left(-\left(\frac{32}{3}l_4\right)-\frac{4}{9}\ln^4 2\right.\\
&+\left((-15+24\ln 2)\zeta_2-\frac{101}{3}\zeta_3+\frac{4337}{324}\right)L_z\\
&-\frac{85}{6}L_z^2+\frac{890}{81}L_z^3\\
&+\left(-6\ln 2+\frac{8}{3}\ln^2 2+\frac{15}{4}\right)\zeta_2\\
&\left.-\frac{47}{6}\zeta_3+\frac{25}{3}\zeta_4+\frac{5}{3}\zeta_5-\frac{16883}{2916}\right)\frac{1}{z^3}\\
&+\left(\left(-2\zeta_3+\frac{757}{972}\right)L_z+\frac{19855}{648}L_z^2-\frac{1345}{81}L_z^3\right.\\
&+(-5+8\ln 2)\zeta_2+\frac{373}{36}\zeta_3-\frac{1760405}{93312}\Bigg)\frac{1}{z^4}\\
&+\left(\left(-\left(\frac{3}{5}\zeta_3\right)+\frac{27867253}{1620000}\right)L_z-\frac{617069}{54000}L_z^2\right.\\
&-\frac{64663}{4050}L_z^3+\left(3\ln 2-\frac{15}{8}\right)\zeta_2+\frac{1306}{675}\zeta_3\\
&\left.+\frac{804239879}{116640000}\right)\frac{1}{z^5}\\
&+\left(\left(-\left(\frac{4}{15}\zeta_3\right)+\frac{36020231}{2430000}\right)L_z-\frac{4796371}{81000}L_z^2\right.\\
&-\frac{50866}{2025}L_z^3+\left(-1+\frac{8}{5}\ln 2\right)\zeta_2+\frac{10987}{900}\zeta_3\\
&\left.+\frac{700685473}{29160000}\right)\frac{1}{z^6}\\
&+\left(\left(-\left(\frac{1}{7}\zeta_3\right)-\frac{7266775483}{121550625}\right)L_z\right.\\
&-\frac{20158677919}{111132000}L_z^2-\frac{3780751}{99225}L_z^3+\left(\ln 2-\frac{5}{8}\right)\zeta_2\\
&+\frac{2673157}{176400}\zeta_3\\
&\left.+\frac{44535682588013}{490092120000}\right)\frac{1}{z^7}\Bigg]+\ldots,
\end{aligned}
$$

$$
\begin{aligned}
\Pi_{FA}^{(2),v}=&\frac{3}{16\pi^2}\left[\frac{18433}{2592}+\frac{4}{3}C_l^2-\left(\frac{11}{4}\frac{1}{\sqrt{3}}C_l\right)+\frac{32}{3}l_4\right.\\
&+\frac{4}{9}\ln^4 2+\left(-\left(\frac{22}{3}\zeta_3\right)+\frac{41}{4}\right)L_z\\
&+\left(-4\ln 2-\frac{8}{3}\ln^2 2+\frac{1985}{648}\right)\zeta_2-\left(\frac{17}{2}\zeta_3\right)\\
&-\left(\frac{41}{6}\zeta_4\right)-\left(\frac{5}{3}\zeta_5\right)+\frac{11}{6}L_z^2\\
&+\left(\frac{39}{8}\sqrt{3}C_l+\frac{3}{4}C_l^2-16l_4-\frac{2}{3}\ln^4 2\right.\\
&+\left((-4+12\ln 2)\zeta_2+\frac{25}{2}\zeta_3-\frac{11}{3}\right)L_z\\
&-\frac{38}{3}L_z^2-\frac{11}{3}L_z^3\\
&+\left(3\ln 2+4\ln^2 2-\frac{97}{24}\right)\zeta_2+12\zeta_3+\frac{427}{32}\zeta_4\\
&\left.-\frac{65}{6}\zeta_5-\frac{4015}{288}\right)\frac{1}{z}\\
&+\left(-\left(\frac{91}{6}L_z\right)+(-4+12\ln 2)\zeta_2+\frac{52}{3}\zeta_3-20\zeta_5\right.\\
&\left.+\frac{1561}{144}\right)\frac{1}{z^2}\\
&+\left(\frac{16}{3}l_4+\frac{2}{9}\ln^4 2+\left((4-12\ln 2)\zeta_2+\frac{13}{2}\zeta_3\right.\right.\\
&\left.-\frac{22153}{1944}\right)L_z+\frac{3409}{324}L_z^2+\frac{143}{81}L_z^3\\
&+\left(-1+3\ln 2-\frac{4}{3}\ln^2 2\right)\zeta_2+\frac{293}{72}\zeta_3-\frac{25}{6}\zeta_4\\
&\left.-\frac{5}{2}\zeta_5+\frac{108761}{23328}\right)\frac{1}{z^3}
\end{aligned}
$$

$$
\begin{aligned}
&+\left(\left(2\zeta_3-\frac{11267}{3888}\right)L_z-\frac{1789}{324}L_z^2+\frac{491}{81}L_z^3\right.\\
&+\left(-4\ln 2+\frac{4}{3}\right)\zeta_2-\frac{80}{9}\zeta_3+\frac{1658717}{186624}\Big)\frac{1}{z^4}\\
&+\left(\left(\frac{3}{5}\zeta_3-\frac{10253071}{1944000}\right)L_z+\frac{43999}{6480}L_z^2\right.\\
&+\frac{331}{45}L_z^3+\left(-\left(\frac{3}{2}\ln 2\right)+\frac{1}{2}\right)\zeta_2\\
&-\frac{20327}{10800}\zeta_3-\frac{69281173}{14580000}\Big)\frac{1}{z^5}\\
&+\left(\left(\frac{4}{15}\zeta_3-\frac{13535191}{2430000}\right)L_z+\frac{40111}{1350}L_z^2\right.\\
&+\frac{2767}{225}L_z^3+\left(-\left(\frac{4}{5}\ln 2\right)+\frac{4}{15}\right)\zeta_2-\frac{5837}{900}\zeta_3\\
&-\frac{120018929}{9720000}\Big)\frac{1}{z^6}\\
&+\left(\left(\frac{1}{7}\zeta_3+\frac{11463009101}{370440000}\right)L_z+\frac{2877743137}{31752000}L_z^2\right.\\
&+\frac{1072571}{56700}L_z^3+\left(-\left(\frac{1}{2}\ln 2\right)+\frac{1}{6}\right)\zeta_2\\
&-\frac{2742577}{352800}\zeta_3-\frac{104055061483}{2286144000}\Big)\frac{1}{z^7}\Big]+\ldots,
\end{aligned}
$$

$$
\begin{aligned}
\Pi_{FL}^{(2),v}=\frac{3}{16\pi^2}&\left[-\frac{589}{216}+\frac{122}{27}\zeta_3+\frac{2}{9}\zeta_2-\left(\frac{2}{3}L_z^2\right)\right.\\
&+\left(\frac{8}{3}\zeta_3-\frac{11}{3}\right)L_z\\
&+\left(\left(-4\zeta_2-4\zeta_3+\frac{7}{3}\right)L_z+\frac{10}{3}L_z^2\right.\\
&+\frac{4}{3}L_z^3+\frac{1}{6}\zeta_2-\frac{22}{3}\zeta_3+\frac{89}{18}\Big)\frac{1}{z}\\
&+\left(\frac{16}{3}L_z-4\zeta_2-\frac{2}{3}\zeta_3-\frac{131}{36}\right)\frac{1}{z^2}\\
&+\left(\left(4\zeta_2+\frac{4}{3}\zeta_3+\frac{2183}{486}\right)L_z-\frac{299}{81}L_z^2-\frac{52}{81}L_z^3\right.\\
&-\zeta_2+2\zeta_3-\frac{11491}{5832}\Big)\frac{1}{z^3}\\
&+\left(-\left(\frac{1625}{648}L_z\right)-\frac{23}{54}L_z^2+\frac{8}{27}L_z^3+\frac{4}{3}\zeta_2+\frac{2}{3}\zeta_3\right.\\
&+\frac{15455}{7776}\Big)\frac{1}{z^4}\\
&+\left(-\left(\frac{199679}{162000}L_z\right)+\frac{497}{2700}L_z^2+\frac{4}{45}L_z^3+\frac{1}{2}\zeta_2\right.\\
&+\frac{1}{5}\zeta_3+\frac{233149}{405000}\Big)\frac{1}{z^5}\\
&+\left(-\left(\frac{19067}{30375}L_z\right)+\frac{41}{225}L_z^2+\frac{16}{405}L_z^3+\frac{4}{15}\zeta_2\right.\\
&+\frac{4}{45}\zeta_3+\frac{3236209}{14580000}\Big)\frac{1}{z^6}\\
&+\left(-\left(\frac{3920897}{11113200}L_z\right)+\frac{247}{1764}L_z^2+\frac{4}{189}L_z^3+\frac{1}{6}\zeta_2\right.\\
&+\frac{1}{21}\zeta_3+\frac{245309459}{2333772000}\Big)\frac{1}{z^7}\Big]+\ldots,
\end{aligned}
$$

$$
\begin{aligned}
\Pi_{FH}^{(2),v}=\frac{3}{16\pi^2}&\left[-\frac{1141}{216}+\frac{410}{27}\zeta_3-\left(\frac{8}{3}\zeta_2\right)\right.\\
&-\left(\frac{2}{3}L_z^2\right)+\left(\frac{8}{3}\zeta_3-\frac{11}{3}\right)L_z-16\frac{1}{\sqrt{3}}C_l\\
&+\left(9\sqrt{3}C_l+\left(8\zeta_2-4\zeta_3-\frac{11}{3}\right)L_z+\frac{10}{3}L_z^2\right.\\
&+\frac{4}{3}L_z^3+2\zeta_2-\frac{20}{3}\zeta_3-\frac{95}{9}\Big)\frac{1}{z}\\
&+\left(\left(-16\zeta_3+\frac{68}{3}\right)L_z-4L_z^2+8\zeta_2\right.\\
&+\frac{22}{3}\zeta_3-\frac{551}{36}\Big)\frac{1}{z^2}\\
&+\left(\left(-8\zeta_2+\frac{4}{3}\zeta_3+\frac{1111}{486}\right)L_z+\frac{173}{27}L_z^2-\frac{20}{9}L_z^3\right.\\
&+2\zeta_2-\frac{32}{27}\zeta_3+\frac{2129}{5832}\Big)\frac{1}{z^3}\\
&+\left(\frac{1177}{216}L_z-\frac{31}{6}L_z^2+\frac{176}{27}L_z^3-\frac{8}{3}\zeta_2\right.\\
&-\frac{4}{3}\zeta_3-\frac{3191}{7776}\Big)\frac{1}{z^4}\\
&+\left(-\left(\frac{136549}{54000}L_z\right)+\frac{6679}{900}L_z^2+\frac{1864}{135}L_z^3-\zeta_2\right.\\
&-\frac{34}{5}\zeta_3-\frac{3922271}{1215000}\Big)\frac{1}{z^5}\\
&+\left(\frac{824581}{121500}L_z+\frac{11756}{225}L_z^2+\frac{8192}{405}L_z^3-\frac{8}{15}\zeta_2\right.\\
&-\frac{1568}{135}\zeta_3-\frac{337954307}{14580000}\Big)\frac{1}{z^6}\\
&+\left(\frac{1750009337}{18522000}L_z+\frac{2488393}{14700}L_z^2+\frac{8264}{315}L_z^3\right.\\
&-\frac{1}{3}\zeta_2-\frac{5078}{315}\zeta_3-\frac{912529125371}{11668860000}\Big)\frac{1}{z^7}\Big]+\ldots,
\end{aligned}
$$

$$
\begin{aligned}
\Pi_{FF}^{(2),s}=\frac{3}{16\pi^2}&\left[\frac{1961}{288}+\frac{3}{2}C_l^2+\frac{39}{4}\sqrt{3}C_l-32l_4\right.\\
&-\left(\frac{4}{3}\ln^4 2\right)+6L_z^3+\frac{57}{4}L_z^2\\
&+\left((-15+24\ln 2)\zeta_2-15\zeta_3+\frac{109}{8}\right)L_z\\
&+\big(30\ln 2+8\ln^2 2\\
&-\frac{1235}{72}\Big)\zeta_2-\left(\frac{631}{12}\zeta_3\right)+\frac{363}{16}\zeta_4+15\zeta_5\\
&+\left(64l_4+\frac{8}{3}\ln^4 2+(-42+(60-96\ln 2)\zeta_2\right.
\end{aligned}
$$

$$
\begin{aligned}
&+72\zeta_3)L_z - 3L_z^2 - 48L_z^3 \\
&+(15 - 24\ln 2 - 16\ln^2 2)\zeta_2 + \frac{137}{2}\zeta_3 \\
&- 50\zeta_4 - 50\zeta_5 + \frac{3}{8}\Bigg)\frac{1}{z} + \Bigg(-32l_4 - \frac{4}{3}\ln^4 2 \\
&+ \Bigg((-45 + 72\ln 2)\zeta_2 - 69\zeta_3 + \frac{299}{4}\Bigg)L_z \\
&- \frac{201}{2}L_z^2 + 78L_z^3 \\
&+ \Bigg(-42\ln 2 + 8\ln^2 2 + \frac{105}{4}\Bigg)\zeta_2 + \frac{51}{2}\zeta_3 \\
&+ 25\zeta_4 + 5\zeta_5 - \frac{237}{8}\Bigg)\frac{1}{z^2} \\
&+ \Bigg(\Bigg(-16\zeta_3 - \frac{2351}{27}\Bigg)L_z + 96L_z^2 - \frac{896}{27}L_z^3 \\
&+ (-10 + 16\ln 2)\zeta_2 - 41\zeta_3 + \frac{137243}{3888}\Bigg)\frac{1}{z^3} \\
&+ \Bigg(\Bigg(-\zeta_3 + \frac{139555}{2592}\Bigg)L_z + \frac{2719}{432}L_z^2 - \frac{575}{54}L_z^3 \\
&+ \Bigg(5\ln 2 - \frac{25}{8}\Bigg)\zeta_2 + \frac{113}{4}\zeta_3 - \frac{1271839}{20736}\Bigg)\frac{1}{z^4} \\
&+ \Bigg(\Bigg(-\Bigg(\frac{2}{5}\zeta_3\Bigg) + \frac{17774837}{1620000}\Bigg)L_z + \frac{63049}{54000}L_z^2 \\
&- \frac{1514}{225}L_z^3 + \Bigg(\frac{12}{5}\ln 2 - \frac{3}{2}\Bigg)\zeta_2 - \frac{809}{200}\zeta_3 \\
&+ \frac{175044221}{19440000}\Bigg)\frac{1}{z^5} \\
&+ \Bigg(\Bigg(-\Bigg(\frac{1}{5}\zeta_3\Bigg) + \frac{5650789}{162000}\Bigg)L_z - \frac{78107}{36000}L_z^2 \\
&- \frac{7247}{675}L_z^3 + \Bigg(\frac{7}{5}\ln 2 - \frac{7}{8}\Bigg)\zeta_2 + \frac{11261}{1200}\zeta_3 \\
&- \frac{2411369}{405000}\Bigg)\frac{1}{z^6} \\
&+ \Bigg(\Bigg(-\Bigg(\frac{4}{35}\zeta_3\Bigg) + \frac{215940050209}{3889620000}\Bigg)L_z \\
&+ \frac{18459061}{9261000}L_z^2 - \frac{70724}{6615}L_z^3 \\
&+ \Bigg(\frac{32}{35}\ln 2 - \frac{4}{7}\Bigg)\zeta_2 + \frac{1261}{588}\zeta_3 \\
&+ \frac{339666207683}{32672808000}\Bigg)\frac{1}{z^7}\Bigg] + \ldots,
\end{aligned}
$$

$$
\begin{aligned}
\Pi_{FA}^{(2),s} = \frac{3}{16\pi^2}\Bigg[&\frac{4783}{288} - \Bigg(\frac{3}{4}C_l^2\Bigg) - \Bigg(\frac{39}{8}\sqrt{3}C_l\Bigg) \\
&+16l_4 + \frac{2}{3}\ln^4 2 + \frac{11}{3}L_z^3 + \frac{71}{3}L_z^2 \\
&+ \Bigg((4 - 12\ln 2)\zeta_2 - \frac{25}{2}\zeta_3 + \frac{98}{3}\Bigg)L_z \\
&+ \Bigg(-15\ln 2 - 4\ln^2 2 + \frac{193}{24}\Bigg)\zeta_2 - \Bigg(\frac{5}{2}\zeta_3\Bigg) \\
&- \Bigg(\frac{427}{32}\zeta_4\Bigg) - \Bigg(\frac{5}{2}\zeta_5\Bigg) + \Bigg(-32l_4 - \frac{4}{3}\ln^4 2 \\
&+ \Bigg((-16 + 48\ln 2)\zeta_2 + 22\zeta_3 - \frac{77}{6}\Bigg)L_z \\
&- \frac{185}{3}L_z^2 - \frac{44}{3}L_z^3 \\
&+(-4 + 12\ln 2 + 8\ln^2 2)\zeta_2 \\
&+ \frac{41}{6}\zeta_3 + 25\zeta_4 + 5\zeta_5 - \frac{821}{72}\Bigg)\frac{1}{z} \\
&+ \Bigg(16l_4 + \frac{2}{3}\ln^4 2 \\
&+ \Bigg((12 - 36\ln 2)\zeta_2 - \frac{25}{2}\zeta_3 - \frac{405}{8}\Bigg)L_z \\
&+ \frac{509}{12}L_z^2 + \frac{55}{3}L_z^3 \\
&+(-7 + 21\ln 2 - 4\ln^2 2)\zeta_2 + \frac{17}{24}\zeta_3 \\
&- \frac{25}{2}\zeta_4 - \frac{15}{2}\zeta_5 + \frac{5239}{288}\Bigg)\frac{1}{z^2} \\
&+ \Bigg(\Bigg(16\zeta_3 + \frac{9395}{324}\Bigg)L_z + \frac{209}{27}L_z^2 - \frac{248}{27}L_z^3 \\
&+ \Bigg(-8\ln 2 + \frac{8}{3}\Bigg)\zeta_2 + 8\zeta_3 - \frac{16153}{972}\Bigg)\frac{1}{z^3} \\
&+ \Bigg(\Bigg(\zeta_3 - \frac{42247}{5184}\Bigg)L_z - \frac{6847}{432}L_z^2 + \frac{193}{27}L_z^3 \\
&+ \Bigg(-\Bigg(\frac{5}{2}\ln 2\Bigg) + \frac{5}{6}\Bigg)\zeta_2 - \frac{725}{48}\zeta_3 + \frac{420179}{15552}\Bigg)\frac{1}{z^4} \\
&+ \Bigg(\Bigg(\frac{2}{5}\zeta_3 - \frac{650497}{162000}\Bigg)L_z - \frac{47}{40}L_z^2 + \frac{427}{135}L_z^3 \\
&+ \Bigg(-\Bigg(\frac{6}{5}\ln 2\Bigg) + \frac{2}{5}\Bigg)\zeta_2 + \frac{118}{75}\zeta_3 - \frac{15978853}{4320000}\Bigg)\frac{1}{z^5} \\
&+ \Bigg(\Bigg(\frac{1}{5}\zeta_3 - \frac{10567931}{648000}\Bigg)L_z + \frac{1979}{2880}L_z^2 + \frac{2833}{540}L_z^3 \\
&+ \Bigg(-\Bigg(\frac{7}{10}\ln 2\Bigg) + \frac{7}{30}\Bigg)\zeta_2 - \frac{3939}{800}\zeta_3 \\
&+ \frac{16344943}{5184000}\Bigg)\frac{1}{z^6} + \Bigg(\Bigg(\frac{4}{35}\zeta_3 \\
&- \frac{3758939963}{138915000}\Bigg)L_z - \frac{13834}{11025}L_z^2 + \frac{24902}{4725}L_z^3 \\
&+ \Bigg(-\Bigg(\frac{16}{35}\ln 2\Bigg) + \frac{16}{105}\Bigg)\zeta_2 - \frac{591}{490}\zeta_3 \\
&- \frac{471073727}{92610000}\Bigg)\frac{1}{z^7}\Bigg] + \ldots,
\end{aligned}
$$

$$
\begin{aligned}
\Pi_{FL}^{(2),s} = \frac{3}{16\pi^2}\Bigg[&-\frac{95}{18} + 6\zeta_3 + \frac{23}{6}\zeta_2 - \Bigg(\frac{4}{3}L_z^3\Bigg) \\
&- \Bigg(\frac{22}{3}L_z^2\Bigg) + \Bigg(4\zeta_2 + 4\zeta_3 - \frac{31}{3}\Bigg)L_z
\end{aligned}
$$

$$
\begin{aligned}
&+\left(\left(-16\zeta_2-8\zeta_3+\frac{14}{3}\right)L_z+\frac{52}{3}L_z^2\right.\\
&+\frac{16}{3}L_z^3-4\zeta_2-\frac{26}{3}\zeta_3+\frac{61}{18}\Big)\frac{1}{z}\\
&+\left(\left(12\zeta_2+4\zeta_3+\frac{27}{2}\right)L_z-\frac{31}{3}L_z^2-\frac{20}{3}L_z^3\right.\\
&-7\zeta_2-\frac{2}{3}\zeta_3-\frac{341}{72}\Big)\frac{1}{z^2}\\
&+\left(-\left(\frac{118}{81}L_z\right)-\frac{136}{27}L_z^2+\frac{64}{27}L_z^3\right.\\
&+\frac{8}{3}\zeta_2+\frac{10}{3}\zeta_3-\frac{191}{486}\Big)\frac{1}{z^3}\\
&+\left(-\left(\frac{4981}{1296}L_z\right)+\frac{143}{108}L_z^2+\frac{4}{27}L_z^3+\frac{5}{6}\zeta_2\right.\\
&+\frac{1}{3}\zeta_3+\frac{6755}{3888}\Big)\frac{1}{z^4}\\
&+\left(-\left(\frac{85273}{81000}L_z\right)+\frac{649}{1350}L_z^2+\frac{8}{135}L_z^3\right.\\
&+\frac{2}{5}\zeta_2+\frac{2}{15}\zeta_3+\frac{1217977}{4860000}\Big)\frac{1}{z^5}\\
&+\left(-\left(\frac{26531}{54000}L_z\right)+\frac{719}{2700}L_z^2+\frac{4}{135}L_z^3+\frac{7}{30}\zeta_2\right.\\
&+\frac{1}{15}\zeta_3+\frac{54839}{540000}\Big)\frac{1}{z^6}\\
&+\left(-\left(\frac{320456}{1157625}L_z\right)+\frac{5693}{33075}L_z^2\right.\\
&+\frac{16}{945}L_z^3+\frac{16}{105}\zeta_2+\frac{4}{105}\zeta_3+\frac{218460799}{3889620000}\Big)\frac{1}{z^7}\Big]\\
&+\ldots,
\end{aligned}
$$

$$
\begin{aligned}
\Pi_{FH}^{(2),s}=\frac{3}{16\pi^2}&\left[-\frac{46}{9}+\frac{64}{3}\zeta_3-10\zeta_2-\left(\frac{4}{3}L_z^3\right)\right.\\
&-\left(\frac{22}{3}L_z^2\right)+\left(-8\zeta_2+4\zeta_3-\frac{13}{3}\right)L_z-9\sqrt{3}C_l\\
&+\left(\left(32\zeta_2-8\zeta_3+\frac{14}{3}\right)L_z+\frac{52}{3}L_z^2+\frac{16}{3}L_z^3\right.\\
&+8\zeta_2+\frac{46}{3}\zeta_3-\frac{191}{18}\Big)\frac{1}{z}\\
&+\left(\left(-24\zeta_2+4\zeta_3+\frac{3}{2}\right)L_z-\frac{13}{3}L_z^2-\frac{20}{3}L_z^3\right.\\
&+14\zeta_2-\frac{20}{3}\zeta_3+\frac{1639}{72}\Big)\frac{1}{z^2}\\
&+\left(-\left(\frac{1826}{81}L_z\right)+\frac{124}{9}L_z^2-\frac{16}{3}\zeta_2\right.\\
&+\frac{14}{9}\zeta_3+\frac{3685}{486}\Big)\frac{1}{z^3}\\
&+\left(\frac{8347}{1296}L_z+\frac{217}{36}L_z^2+\frac{8}{9}L_z^3-\frac{5}{3}\zeta_2\right.\\
&+\frac{26}{9}\zeta_3-\frac{34093}{3888}\Big)\frac{1}{z^4}\\
&+\left(\frac{752611}{81000}L_z+\frac{3683}{450}L_z^2+\frac{272}{45}L_z^3\right.\\
&-\frac{4}{5}\zeta_2-\frac{44}{45}\zeta_3-\frac{34816841}{4860000}\Big)\frac{1}{z^5}\\
&+\left(\frac{3698791}{162000}L_z+\frac{34153}{900}L_z^2+\frac{1528}{135}L_z^3\right.\\
&-\frac{7}{15}\zeta_2-\frac{74}{15}\zeta_3-\frac{29545141}{1620000}\Big)\frac{1}{z^6}\\
&+\left(\frac{378496261}{3472875}L_z+\frac{491947}{3675}L_z^2+\frac{15712}{945}L_z^3\right.\\
&-\frac{32}{105}\zeta_2-\frac{312}{35}\zeta_3-\frac{74992868899}{1296540000}\Big)\frac{1}{z^7}\Big]+\ldots
\end{aligned}
$$

In the above expressions the following symbols have been used: $l_4=\mathrm{Li}_4(1/2)$, $C_l=\mathrm{Cl}_2(\pi/3)=\mathrm{Im}[\mathrm{Li}_2(\exp(\mathrm{i}\pi/3))]$, $\zeta_2=\pi^2/6$, $\zeta_3\approx 1.202057$, $\zeta_4=\pi^4/90$, $\zeta_5\approx 1.036928$ and $L_z=-(\ln(-z))/2$. A Mathematica input can be found under the URL
http://www-ttp.physik.uni-karlsruhe.de/Progdata/ttp01/ttp01-14.

References

1. K.G. Chetyrkin, J.H. Kühn, M. Steinhauser, Phys. Lett. B **371**, 93 (1996); Nucl. Phys. B **482**, 213 (1996); Nucl. Phys. B **505**, 40 (1997)
2. K.G. Chetyrkin, R. Harlander, M. Steinhauser, Phys. Rev. D **58**, 014012 (1998)
3. K.G. Chetyrkin, M. Steinhauser, Phys. Lett. B **502**, 104 (2001)
4. D.J. Broadhurst, A.G. Grozin, Phys. Lett. B **274**, 421 (1992)
5. E. Bagan, P. Ball, V.M. Braun, H.G. Dosch, Phys. Lett. B **278**, 457 (1992)
6. K. Schilcher, M.D. Tran, N.F. Nasrallah, Nucl. Phys. B **181**, (1981); B **187**, 594(E) (1981)
7. D.J. Broadhurst, Phys. Lett. B **101**, 423 (1981)
8. T.H. Chang, K.J. Gaemers, W.L. van Neerven, Nucl. Phys. B **202**, 407 (1982)
9. L.J. Reinders, H. Rubinstein, S. Yazaki, Phys. Lett. B **97**, 257 (1980), B **100**, 519(E) (1981), B **103**, 35 (1981)
10. A. Djouadi, P. Gambino, Phys. Rev. D **49**, 3499 (1994)
11. P.A. Baikov, D.J. Broadhurst, 4th International Workshop on Software Engineering and Artificial Intelligence for High Energy and Nuclear Physics (AIHENP95), Pisa, Italy, 3–8 April 1995, published in Pisa AIHENP (1995) 167
12. R.V. Harlander, Report No.: hep-ph/0102266
13. See, e.g., V.A. Smirnov, Mod. Phys. Lett. A **10**, 1485 (1995)
14. J. Fleischer, O.V. Tarasov, Z. Phys. C **64**, 413 (1994)
15. D.J. Broadhurst, A.G. Grozin, Phys. Rev. D **52**, 4082 (1995)
16. A.G. Grozin, Phys. Lett. B **445**, 165 (1998)
17. X. Ji, M.J. Musolf, Phys. Lett. B **257**, 409 (1991); D.J. Broadhurst, A.G. Grozin, Phys. Lett. B **267**, 105 (1991); V. Giménez, Nucl. Phys. B **375**, 582 (1992)

18. K.G. Chetyrkin, M. Steinhauser, unpublished
19. P. Nogueira, J. Comput. Phys. **105**, 279 (1993)
20. R. Harlander, Ph.D. thesis, University of Karlsruhe (Shaker Verlag, Aachen 1998)
21. Th. Seidensticker, Diploma thesis (University of Karlsruhe, 1998), unpublished
22. M. Steinhauser, Comput. Phys. Commun. **134**, 335 (2001)
23. S.A. Larin, F.V. Tkachov, J.A.M. Vermaseren, Rep. No. NIKHEF-H/91-18 (Amsterdam, 1991)
24. R. Harlander, M. Steinhauser, Prog. Part. Nucl. Phys. **43**, 167 (1999)
25. M.C. Smith, S. Willenbrock, Phys. Rev. D **54**, 6696 (1996)
26. R. Hamberg, W. van Neerven, T. Matsuura, Nucl. Phys. B **359**, 343 (1991); W. van Neerven, E. Zijlstra, Nucl. Phys. B **382**, 11 (1992)
27. A.D. Martin, R.G. Roberts, W.J. Stirling, R.S. Thorne, Eur. Phys. J. C **18**, 117 (2000)
28. J.F. Gunion, H.E. Haber, G. Kane, S. Dawson, The Higgs hunter's guide (Addison Wesley 1990)
29. K.G. Chetyrkin, J.H. Kühn, M. Steinhauser, Comput. Phys. Commun. **133**, 43 (2000)